Dynamical studies of chemical reactions relevant to the local atmosphere of the orbiting Space Shuttle

Prof. Piergiorgio Casavecchia (*Principal Investigator*)

Dipartimento di Chimica
Università di Perugia
Via Elce di Sotto, 8
06123 Perugia
Italy
Phone: (75) 585-5514
Fax: (75) 585-5606

SPC-94-4042

THIRD YEAR FINAL REPORT

Period covered
1 July 1996 - 30 June 1997 (extended to 31 December 1997)

Third Year Final Report
(1 July 1996 - 31 December 1997)

Abstract

We have concluded, within the three year contract (1 July 1994 - 30 June 1997, extended until 31 December 1997), the investigation of the dynamics of a series of elementary chemical reactions of atoms ($O(^3P,^1D)$ and $N(^2D)$) and radicals ($OH(^2\Pi)$) relevant to the local atmosphere of the Space Shuttle in low Earth orbit. The technique employed was the crossed molecular beams scattering method with mass spectrometric detection. Specifically, during the third year of the research project we have:

1) Extended further the investigation of the important reaction $O(^1D)+H_2$ by performing measurements of reactive differential cross sections at more collision energies, stimulated by recent theoretical developments (i.e. the calculation of new accurate potential energy surfaces and new dynamical predictions on these surfaces).
2) Carried out the investigation of the important reactions of electronically excited N atoms, $N(^2D)$, with molecular hydrogen, acetylene and ethylene. These reactions were studied in substitution of the initially planned reactions of the NH radical.
3) Studied the reactions $O(^3P,^1D)+CH_3I$ to explore the role of nonadiabatic effects (inter-system crossing) in the dynamics of atomic oxygen reactions. These reactions were studied in substitution of those of $O(^1D)+CH_4$ and $O(^1D)+H_2O$ which, for technical difficulties, could not be investigated.
4) Constructed a second radio-frequency discharge beam source which will allow us to study the dynamics of radical-radical reactions in the next future.

During the overall three years period of the contract, we have therefore studied the following reactions :

1) $OH + CO \rightarrow CO_2 + H$
2) $OH + H_2 \rightarrow H_2O + H$
3) $O(^1D) + H_2 \rightarrow OH + H$
4) $O(^3P,^1D) + CH_3I \rightarrow IO + CH_3$
5) $N(^2D) + H_2 \rightarrow NH + H$
6) $N(^2D) + C_2H_2 \rightarrow HCCN + H$
7) $N(^2D) + C_2H_4 \rightarrow CH_3CN + H$

Reactions (1)-(3), and presumably also reactions (5) and (6), occur in the local atmosphere of the orbiting Space Shuttle. Their reaction dynamics have been elucidated in detail by measuring reactive differential cross sections in crossed molecular beam scattering experiments. It has been shown that OH radicals from $O(^1D)+H_2$, NH radicals from $N(^2D)+H_2$, HCCN radicals from $N(^2D)+C_2H_2$, and H_2O molecules from $OH+H_2$ are formed highly vibrationally excited and therefore give rise to strong emission in the infrared. This information is particularly relevant for a detailed understanding and modeling of the local atmosphere of the orbiting Space Shuttle. CO_2 from reaction (1) is instead found to be formed translationally very excited, rotationally excited and, hence, vibrationally cold. The study of reaction (4) has shown that triplet-singlet inter-system-crossing occurs with very high probability when a heavy atom such as iodine is involved.

REPORT DOCUMENTATION PAGE

Form Approved OMB No. 0704-0188

1. AGENCY USE ONLY (Leave blank)	2. REPORT DATE	3. REPORT TYPE AND DATES COVERED
	February 1998	Final Report

4. TITLE AND SUBTITLE

Dynamical Studies Of Chemical Reactions Relevant To The Local Atmosphere Of The Orbiting Space Shuttle

5. FUNDING NUMBERS

F6170894C0013

6. AUTHOR(S)

Dr. Piergiorgio Casavecchia

7. PERFORMING ORGANIZATION NAME(S) AND ADDRESS(ES)

Dipartimento di Chimica, University of Perugia
via Elce di Sotto, 8
Perugia 06123
Italy

8. PERFORMING ORGANIZATION REPORT NUMBER

N/A

9. SPONSORING/MONITORING AGENCY NAME(S) AND ADDRESS(ES)

EOARD
PSC 802 BOX 14
FPO 09499-0200

10. SPONSORING/MONITORING AGENCY REPORT NUMBER

SPC 94-4042

11. SUPPLEMENTARY NOTES

12a. DISTRIBUTION/AVAILABILITY STATEMENT

Approved for public release; distribution is unlimited.

12b. DISTRIBUTION CODE

A

13. ABSTRACT (Maximum 200 words)

This report results from a contract tasking Dipartimento di Chimica, University of Perugia as follows: The contractor will measure differential cross sections for reactions of O(3P), O(1D) and OH(2P) with various radials and molecules present in the local atmosphere of the space shuttle in low earth orbit as described in the original proposal for this work.

14. SUBJECT TERMS

Nil

15. NUMBER OF PAGES

44

16. PRICE CODE

N/A

17. SECURITY CLASSIFICATION OF REPORT	18. SECURITY CLASSIFICATION OF THIS PAGE	19. SECURITY CLASSIFICATION OF ABSTRACT	20. LIMITATION OF ABSTRACT
UNCLASSIFIED	UNCLASSIFIED	UNCLASSIFIED	UL

In most cases the experimental results have been compared, within fruitful collaborations, with state-of-the-art dynamical calculations (quasiclassical and/or quantum) on *ab initio* potential energy surfaces.

The information obtained from the study of the above reactive collisions at the microscopic level, besides their interest from a fundamental point of view, will enable the world scientific community and the U.S. Air Force to better understand the local environment of measuring platforms in space and may also be useful for the improvement of the SOCRATES code, aimed at assessing the effects of contamination on measurements aboard spacecrafts in low Earth orbit.

A detailed report on reaction (1), in which experimental results and theoretical predictions are compared, has been published in a chapter in *Advanced Series in Chemical Physics, vol. 6 "The Chemical Dynamics and Kinetics of Small Radicals"* (Publication n. 1).

A detailed combined experimental and theoretical study of reaction (2) has been published in *Chemical Physics* (Publication n. 2).

A comprehensive publication on reactions (3) is currently in press in the *Journal of Chemical Physics* (Publication n. 3) and some results will appear as *Comments to the Faraday Discussion no. 108* on "The Dynamics of Electronically Excited States" (Publications n. 4 and 5).

The development and characterization by Stern-Gerlach magnetic analysis of intense supersonic beams of ground and electronically excited oxygen and nitrogen atoms, $O(^3P, ^1D)$ and $N(^4S, ^2D)$, as well as of $Cl(^2P_{3/2,1/2})$ has been published in *Israel Journal of Chemistry* (special issue on "Molecular beams") (Publication n. 6).

A publication on reactions (4) is currently in preparation (Publication n. 7), while a first partial report will appear as a *Comment to the Faraday Discussion no. 108* on "The Dynamics of Electronically Excited States" (Publication n. 8).

A publication is in preparation on reaction (5) in collaboration with theoretical groups, in which the experimental results are compared with dynamical predictions on a high quality *ab initio* potential energy surface (Publication n. 9). A preliminary report will appear as a *Comment to the Faraday Discussion no. 108* on "The Dynamics of Electronically Excited States" (Publication n. 10).

A publication is also in preparation on reaction (6) (Publication n. 11) for which, again, a preliminary report will appear as a *Comment to the Faraday Discussion no. 108* on "The Dynamics of Electronically Excited States" (Publication n. 12).

A publication is being planned also on reaction (7) (Publication n. 13).

In addition, acknowledgments to AFOSR and EOARD is also made in a series of publications on related reactions (Publications 14-19).

Finally, the above results have also been presented, during the last three years, in numerous (more than ten) Invited Lectures, as well as in many poster contributions, at international conferences.

List of publications on work pertinent to the contract:

1. P. Casavecchia, N. Balucani, and G.G. Volpi
Reactive Scattering of $O(^3P, ^1D)$, $Cl(^2P)$ and OH Radicals

Advanced Series in Physical Chemistry - Vol. 6: *The Chemical Dynamics and Kinetics of Small Radicals*, eds. K. Liu and A.Wagner (World Scientific, Singapore, 1995), cap. 9 (pp. 365-437).

2. M. Alagia, N. Balucani, P. Casavecchia, D. Stranges, G.G. Volpi, D.C. Clary, A. Kliesch, and H.-J. Werner
   The dynamics of the reaction OH + D_2 → HOD + D: Crossed beam experiments and quantum mechanical scattering calculations on *ab initio* potential energy surfaces
   Chemical Physics **207,** 389-409 (1996).
3. M. Alagia, N. Balucani, L. Cartechini, P. Casavecchia, E.H. van Kleef, G.G. Volpi, P.J. Kuntz, and J.J. Sloan
   Crossed molecular beam and quasiclassical trajectory studies of the dynamics of the $O(^1D)+H_2(D_2)$ reaction.
   Journal of Chemical Physics, (submitted 8 October 1997), in press.
4. P. Casavecchia, M. Alagia, N. Balucani, L. Cartechini, E.H. van Kleef, G.G. Volpi, P.J. Kuntz, and J.J. Sloan
   On "Crossed beams and quasiclassical trajectory studies of the $O(^1D)+H_2(D_2)$ reaction"
   Comment to Faraday Discussion no. 108 (University of Sussex, Brighton, U.K., Dec. 15-17, 1997), in press.
5. P. Casavecchia, M. Alagia, N. Balucani, L. Cartechini, E.H. van Kleef, G.G. Volpi, L. Harding, H. Rabitz, T. Hollebeek, T.-S. Ho, L.A. Pederson, and G.C. Schatz
   On "Comparison between experimental differential cross sections and quasiclassical trajectory calculations on ground and excited *ab initio* potential energy surfaces for the $O(^1D)+H_2$ reaction"
   Comment to Faraday Discussion no. 108 (University of Sussex, Brighton, U.K., Dec. 15-17, 1997), in press.
6. M. Alagia, V. Aquilanti, D. Ascenzi, N. Balucani, D. Cappelletti, L. Cartechini, P. Casavecchia, F. Pirani, G. Sanchini, and G.G. Volpi
   Magnetic analysis of supersonic beams of atomic oxygen, nitrogen, and chlorine generated from a radio-frequency discharge.
   Israel Journal of Chemistry (Issue on Molecular Beams) 36, xxx (1997).
7. M. Alagia, N. Balucani, L. Cartechini, P. Casavecchia, M.C. van Beek, and G.G. Volpi
   A crossed molecular beam study of the reactions $O(^3P,^1D)+CH_3I \rightarrow IO+CH_3$: the role of inter-system-crossing.
   Journal of Chemical Physics, in preparation.
8. P. Casavecchia, M. Alagia, N. Balucani, L. Cartechini, M.C. van Beek, and G.G. Volpi
   On "Non-adiabatic effects on the reaction dynamics of atomic oxygen: A crossed beam study of $O(^3P,^1D)+CH_3I$"
   Comment to Faraday Discussion no. 108 (University of Sussex, Brighton, U.K., Dec. 15-17, 1997), in press.
9. M. Alagia, N. Balucani, L. Cartechini, P. Casavecchia, G.G. Volpi, L. Pederson, G. Lendway, G.C. Schatz, L. Harding, H. Rabitz, and T. Takayanagi

Dynamics of the simplest nitrogen atom reaction, $N(^2D)+H_2 \rightarrow NH+H$: A combined experimental and theoretical study.
Science, in preparation.

10. P. Casavecchia, M. Alagia, N. Balucani, L. Cartechini, G.G. Volpi, G.C. Schatz, L. Pederson, G. Lendway, L.R. Harding, T. Hollebeek, H. Rabitz, and T. Takayanagi
On "Crossed beam studies of the reaction of electronically excited ^2D nitrogen atoms with H_2 and comparison with quasiclassical trajectory calculations on an *ab initio* potential energy surface".
Comment to Faraday Discussion no. 108 (University of Sussex, Brighton, U.K., Dec. 15-17, 1997), in press.
11. M. Alagia, L. Cartechini, P. Casavecchia, E.H. van Kleef, G.G. Volpi
Crossed molecular beam studies of the reaction dynamics of electronically excited nitrogen atoms: $N(^2D)$ + acetylene.
Journal of Chemical Physics, in preparation.
12. P. Casavecchia,M. Alagia, N. Balucani, L. Cartechini, E.H. van Kleef, G.G. Volpi
On "The reaction dynamics of electronically excited ^2D atoms with polyatomic molecules: A crossed beam study of $N(^2D)$ + acetylene and ethylene".
Comment to Faraday Discussion no. 108 (University of Sussex, Brighton, U.K., Dec. 15-17, 1997), in press.
13. M. Alagia, N. Balucani, L. Cartechini, P. Casavecchia, and G.G. Volpi
Crossed molecular beam studies of the reaction $N(^2D)$ + ethylene.
Journal of Chemical Physics, in preparation.

List of publications (continued) on related work also containing Acknowledgments to AFOSR and EOARD:

14. M. Alagia, N. Balucani, L. Cartechini, P. Casavecchia, D. Stranges, and G.G. Volpi
Reaction dynamics of three-atom and four-atom systems
in: *Springer Series in Chemical Physics, Volume 61 "Gas-Phase Chemical Reaction Systems", Eds. J. Wolfrum, H.-R. Volpp, R. Rannacher, and J. Warnatz (Springer-Verlag, Heidelberg, 1996), pp. 96-107.*
15. M. Alagia, N. Balucani, P. Casavecchia, A. Laganà, G. Ochoa de Aspuru, E.H. van Kleef, G.G.Volpi, and G. Lendway
On the dynamics of the $O(^1D)+CF_3Br$ reaction
Chemical Physics Letters, **258,** 323-329 (1996).
16. M. Alagia, N. Balucani, L. Cartechini, P. Casavecchia, E.H. van Kleef, G.G. Volpi, F.J. Aoiz, L. Banares, D.W. Schwenke, T.C. Allison, S.L. Mielke, and D.G. Truhlar
Dynamics of the simplest chlorine atom reaction: An experimental and theoretical study
Science **273**, 1519-1522 (1996).
17. M. Alagia, N. Balucani, P. Casavecchia, and G.G. Volpi
A crossed molecular beam study of the reaction $O(^1D)+HI \rightarrow IO+H$
Journal of Physical Chemistry A, **101**, 6455-6462 (1997).
18. D.J. Garton, T.K. Minton, M. Alagia, N. Balucani, P. Casavecchia, and G.G. Volpi
Reactive scattering of ground state and electronically excited oxygen atoms on a liquid hydrocarbon surface.
Faraday Discussion **108**, xxx (1997).

19. M. Alagia, N. Balucani, L. Cartechini, P. Casavecchia, E.H. van Kleef, G.G. Volpi, F.J. Aoiz, L. Banares, D.W. Schwenke, T.C. Allison, S.L. Mielke, and D.G. Truhlar **The dynamics of the reaction Cl + $H_2(D_2)$ → HCl(DCl) + H(D): A Crossed beams, quasiclassical trajectory, and quantum mechanical scattering study.** *J. Phys. Chem. A , in preparation.*

Third Year Report

(1 July 1996 - 31 December 1997)

During the 3rd year of the research project, the plan was to extend the same type of measurements carried during the 1st and 2nd year on the reactions $O(^1D)+H_2(D_2)$, $OH+H_2$, OH+CO, and $N(^2D)+C_2H_2$ to also other systems of relevance in the local atmosphere of the orbiting space shuttle. Specifically, we have:

1) Completed the investigation of the important reaction $O(^1D)+H_2$ by performing measurements of reactive differential cross sections at more collision energies, stimulated by recent theoretical developments (i.e., the calculation of a new accurate potential energy surface (PES) and new theoretical predictions on this PES).
2) Studied the reactions $O(^3P, ^1D) + CH_3I$.
3) Characterized in detail our supersonic beams of atomic oxygen, nitrogen and chlorine by using the Stern-Gerlach magnetic analysis technique.
4) Completed the investigation of the important reactions of electronically excited N atoms, $N(^2D)$, with H_2 and acetylene.
5) Extended the study of $N(^2D)$ reactions to $N(^2D)$ + ethylene.
6) Built a second radio-frequency (RF) discharge beam source to study the dynamics of radical-radical reactions in the next future.

The reactions $O(^3P,^1D) + CH_3I$ were studied in substitution of the reactions $O(^1D)+H_2O$ and $O(^1D)+CH_4$, originally planned, but which could not be investigated due to technical difficulties.[1] The $O(^3P, ^1D) + CH_3I$ system allowed us to explore the effect of electronic excitation and nonadiabatic effects (inter-system crossing) in the dynamics of atomic oxygen reactions, a subject of practical as well as fundamental interest (in this respect it can be regarded as a prototype reaction).

The investigation of $N(^2D)$ reactions, originally not planned, as those with H_2 C_2H_2, and C_2H_4, was carried out to compensate for the fact that, due to technical difficulties encountered during the preliminary experiments aimed at the generation of supersonic beams of NH radicals and to the limited remaining amount of time, we could not pursue the investigation of the dynamics of the reaction NH + NO.

The results obtained during the 3rd year of the contract can be summarized as follows.

$O(^1D) + H_2$

The $O(^1D) + H_2 \rightarrow OH + H$ reaction has attracted over the years a large attention, both experimentally and theoretically, due to its fundamental importance in combustion and atmospheric chemistry, and to the fact that it constitutes a prototype for reactions involving a strongly bound intermediate. For some time this reaction has been thought to be a typical insertion reaction occurring on the ground state PES (corresponding to the ground state of H_2O). But, recently, this notion has been challenged by new experimental and theoretical evidence from our and other

laboratories. Indeed, during the last two years an unprecedented renewed interest has arisen around this system. Experimentally, it has come under investigation at Oxford[2] where by using polarized-laser-photolysis and polarized-sub-Doppler-LIF detection in a bulb state-selected energy-averaged differential cross sections for some specific rovibrational states were derived, at Taiwan[3] where by using Doppler shift techniques and Doppler-selected time-of-flight methods and H(D)-atom REMPI detection differential cross sections were derived, at Boulder[4] where new rate constants were measured, at Heidelberg[5] where integral reaction cross sections were determined, and at Berkeley[6] where differential cross sections are being derived by using ion-imaging techniques. Theoretically, the reaction has been investigated at Northwestern University[7], Princeton[7], Argonne[7], New York[8], Chicago[9], Coimbra[10], Birmingham[11], and Madrid[2] at the level of both electronic structure calculations (to derive improved potential energy surfaces) and dynamical calculations, either by quasiclassical trajectories and approximate quantum methods. A central issue in most of these investigations has been the role and contribution of excited electronic states. This point has been in particular addressed by Schatz and coworkers[7,12], who have presented detailed studies of the $O(^1D)+H_2$ reaction. However, despite the vast amount of work, the mechanism and dynamics of the reaction are still not well understood.

The $O(^1D) + H_2$ reaction was studied at two collision energies (E_c=3.0 and 4.0 kcal/mol) during the first year of this project. Further work on this reaction during the second year was prompted by (i) the observation of a small contamination by H_2O and OH radicals (and/or by ^{17}O and ^{18}O natural abundance) in the $O(^1D)$ beam which had to be accounted for and (ii) by a renewed experimental and theoretical interest on this fundamental system. The amount of correction for $O(^1D)+H_2$ was quantified by measuring the elastic scattering at m/e=16 from H_2 and by determining the ratio (m/e=17)/(m/e=16) by measuring the scattered signal at m/e=17 and m/e=16 from He. The correction turned out to be significant only at small scattering angles, close to the $O(^1D)$ beam; the maximum value being of about 10% at the smallest angle (Θ=5°) and then rapidly decreasing to zero at $\Theta\approx$15°. Stimulated by very recent, accurate calculations of the ground and excited PES and by dynamical calculations on these PES[7,12], we have carried out more crossed beam experiments at different collision energies on $O(^1D)+H_2$ and on the isotopic variant $O(^1D)+D_2$ and have examined the results at the light of the most recent theoretical developments. On the whole, we have measured product and angular velocity distributions in the laboratory frame for $O(^1D)+H_2$ at E_c=0.88, 1.9 and 3.0 kcal/mol and for $O(^1D)+D_2$ at E_c=5.3 and 6.1 kcal/mol (see Fig. 1), and have derived center-of-mass (c.m.) product translational energy and angular distributions (The reaction with D_2 was studied using a beam of $^{18}O(^1D)$, which allowed to detect the OD product at *m/e*=20, which is free of any contamination).[13] The c.m. angular distributions are nearly backward-forward symmetric, but exhibit a slight forward bias at the lowest E_c and a slight backward bias which increases with collision energy at the other E_c (see Fig. 2). About 30% of the total available energy is found to be channeled into product translational energy. We have compared[13] the experimental results with those of quasiclassical trajectory (QCT) calculations (in collaboration with the group of Prof. J.J. Sloan, Univ. of Waterloo, Canada) on the ground state DIM (diatomic-in-molecule) potential energy surface of Kuntz et al.[14] These calculations, carried out at some of the energies, find the product c.m. angular distributions to be backward-forward symmetric in the investigated energy range. This translate into lab

angular distributions which exhibit an asymmetry (because of the c.m.-lab Jacobian transformation) opposite to that experimentally observed, as can be seen from Fig. 1. Interestingly, very recently Schatz and coworkers[12] have shown that the DIM ground state PES is essentially correct and have shown that it predicts symmetric angular distributions, reflecting an insertion dynamics, similar to those predicted by the new RKHS surface, which is based on accurate *ab initio* calculations. Therefore, we attribute the onset of a preferential backward scattering at energies ≥1.9 kcal/mol to the onset of a second micromechanism, a direct abstraction mechanism evolving on one or both of the excited (1A" and 2A') potential energy surfaces, which for collinear geometry are degenerate and are calculated to have a barrier of 2.4 kcal/mol (see below). Our results are in line with recent work by Liu and coworkers[3] who find a preferred backward scattering in the reaction $O(^1D)+HD$ at E_c=4.55 kcal/mol which is not consistent with a simple insertion mechanism on the ground state 1A' PES : a component of abstraction in the dynamics was invoked; in addition, measurements of the excitation function[3] have suggested a barrier of 1.5 kcal/mol for the abstraction channel in the reaction $O(^1D)+H_2$. These results and our finding of a preferred backward scattering already at E_c=1.9 kcal/mol suggest that the abstraction barrier in the new *ab initio* PES is perhaps slightly too high.

It is interesting to note that the QCT calculations of Schatz et al.[7,12] show that the ground state 1A' PES gives a symmetric angular distribution, while the excited 1A" PES gives a backward peaked angular distribution : the global (1A' + 1A") angular distributions for $O(^1D)+H_2$ at E_c=2.7 and 5.0 kcal/mol result to be asymmetric with a backward bias, in line with our findings. Also, the average fraction of energy in translation is calculated by Schatz et al.[12] to be about 33% at E_c=5.0 kcal/mol, which compares well with the value of about 30% determined in our experiments at slightly lower E_c. It seems that the new PES of Schatz et al. should be able to describe the dynamic of the $O(^1D)+H_2$ reaction quite well.

Fig. 3 depicts a schematic correlation diagram of the PES which shows the two possible reaction pathways according to the new *ab initio* calculations[7,12]: on the ground state PES ($^1\Sigma$ and $1A^1$ in $C_{\infty v}$ and C_{2v} geometry, respectively) insertion of $O(^1D)$ into the H_2 bond takes place without energy barrier (for linear approach the barrier is 0.7 kcal/mol) ; on the excited 1A" PES the reaction path is linear with a barrier of 2.4 kcal/mol. The 1A" PES correlates adiabatically with ground state $OH(^2\Pi)+H$, while the other Renner-Teller component of $^1\Pi$, the 2A' PES, can only contribute via surface hopping to ground state products, since it adiabatically leads to $OH(^2\Sigma)+H$. From measurements of angular and velocity distributions of the OD product from the reaction $O(^1D)+D_2$ at E_c=5.3 kcal/mol we have derived the c.m. angular distribution depicted in Fig. 4. This is compared with the results of QCT calculations by Schatz et al. on both the ground state 1A' and excited state 1A" surfaces.[15] As can be seen, the 1A' PES gives an angular distribution which is backward-forward symmetric and reflects an insertion dynamics, while the 1A" PES gives a strongly backward peaked angular distribution as one would expect for a direct abstraction process. Assuming that the reaction proceeds adiabatically on both surfaces, a summed contribution (shown in Fig. 4 as 1A'+1A") is obtained which exhibits a backward biased angular distribution in fairly good agreement with experiment. The role of the other excited 2A' PES (see Fig. 3) needs still to be taken into account, but it is expected to contribute considerably less than 1A" and its

angular distribution is likely to be relatively flat versus θ.[12] It appears that dynamical calculations which take into account both the ground state surface (which has no energy barriers to insertion) and the excited 1A" surface (which has a barrier of 2.4 kcal/mol to collinear abstraction) are able to account nearly quantitatively for the experimental backward peaked OD angular distribution measured for the $O(^1D)+D_2$ reaction at E_c=5.3 kcal/mol. The abstraction pathway is shown[7,12] to give highly vibrationally excited OH product, which summed to the vibrational distribution obtained from the insertion pathway leads to theoretical results which are in line with experimental observation from infrared chemiluminescence experiments.[16]

Although exact quantum scattering calculations need to be performed for an accurate assessment of the new PES, we feel that the most recent theoretical work has led to an improved, though still not fully quantitative, comparison with experiment and then we have now a better understanding of the dynamics of the $O(^1D)+H_2$ reaction.

We can conclude that the $O(^1D)+H_2$ reaction, which occurs in the local atmosphere of the orbiting space shuttle and is also the main source of OH radicals in the stratosphere, takes place through a direct-insertion mechanism at low collision energies (<2 kcal/mol), forming a highly excited H_2O molecule intermediate, which is very short lived and dissociates within a few bending vibrations, before the energy can randomize ; the OH angular distribution is symmetric. At energies above 2 kcal/mol a direct abstraction mechanism on the excited PES starts to contribute producing OH highly vibrationally excited (v'=3 and 4 are predicted[7,12] to be the most populated states of OH) and leading to a preferred backward scattering of the OH product (with respect to the direction of the incoming $O(^1D)$). The high degree of vibrational excitation of the OH product, up to the limit of energy conservation, clearly indicates that the OH radical formed from the $O(^1D)+H_2$ reaction is optically very active and therefore strong emission in the infrared is to be expected. This needs to be taken into account when modeling the local atmosphere of the Space Shuttle orbiting around the Earth.

$O(^3P, ^1D) + CH_3I$

The reactions of atomic oxygen, both in the ground-state $O(^3P)$ and the first electronically excited state $O(^1D)$, with halogenated compounds are of interest in determining the impact of anthropogenic surface release of halogen containing molecules on the atmosphere and especially on the ozone natural balance. They are also of relevance in the combustion chemistry of halogenated compounds, as for instance in their use as fire extinguishers. While the active forms of chlorine and bromine contribute to *stratospheric ozone* depletion, it has been suggested that the *tropospheric ozone* balance may be affected significantly by iodine compounds. Recently, it has been proposed that iodine could account also for the observed depletion of lower stratospheric ozone (below 20 km, altitudes where chlorine and bromine are not very effective for ozone destruction in contrast to iodine) at midlatitudes.[17] The main source of atmospheric iodine is natural (methyl iodide, chloroiodo-methane and diiodomethane are massively produced as metabolic by-products of marine biota), but now iodine containing molecules are also considered as potential substitutes for halon fire suppressants. Although CH_3I has a short lifetime in the atmospheric environment due to its rapid photo-decomposition, it is interesting to probe its reactivity with atmospheric atomic and radical species, such as

$O(^3P)$ and also $O(^1D)$ which is abundant and very active in the ozonosphere. Moreover, the reaction can be regarded as prototypical of the reactions of $O(^3P,^1D)$ with simple iodine containing molecules and their study allows to investigate the role of electronic excitation in reaction dynamics and to explore the possible role of inter-system crossing (ISC) between triplet and singlet potential energy surfaces (see Fig. 5).

Thermodinamically allowed products for the reaction $O(^3P) + CH_3I$ are:

$$\begin{aligned} O(^3P) + CH_3I &\rightarrow IO + CH_3 \quad (1a)\\ &\rightarrow OH + CH_2I \quad (1b)\\ &\rightarrow H + I + CH_2O \quad (1c)\\ &\rightarrow I + CH_3O \quad (1d)\\ &\rightarrow HI + CH_2O \quad (1e) \end{aligned}$$

while the list is even larger for $O(^1D)+CH_3I$, including also formation of $HOI+CH_2$ and ICH_2O+H.

Measurements of the absolute rate constants between 213 and 364 K and product yields at 298 K have been recently reported for the $O(^3P)+CH_3I$ reaction.[18] The $IO+CH_3$ and $OH+CH_2I$ channels were found to account for 44% and 16% of the global rate constant, respectively; product yields for the minor channels are reported to be ~7% for H formation, <3% for CH_3O formation, and <5% for HI formation. While in the similar reaction $O(^3P)+CF_3I$ the formation of IO is largely the dominant reaction channel, the observation of numerous products suggest that the $O(^3P)+CH_3I$ reaction is much more complex and occurs on multiple potential energy surfaces. No dynamical information was available on this system. The rate constant for the reaction $O(^1D)+CH_3I$ has never been determined; however, recent kinetic studies provided room temperature rate constants for the analogous reactions $O(^1D)+CH_3Cl$ and $O(^1D)+CH_3Br$ which are $1.9\cdot10^{-10}$ and $1.8\cdot10^{-10}$ cm^3 $molecule^{-1}$ s^{-1}, respectively.[19] The IO forming channel is expected to be the dominant reaction pathway also for the $O(^1D)$ reaction.

A very interesting issue is the extent of the coupling between the triplet and singlet potential energy surfaces over which the reaction can evolve. A crossing between triplet and singlet PES always occurs in $O(^3P,^1D)$ reactive systems since $O(^1D)$ is higher in energy than $O(^3P)$ by about 2 eV and the most stable intermediate is always a singlet species (see Fig. 5).

Critical for the study of the $O(^3P,^1D)+CH_3I$ reactions by the crossed molecular beam scattering method has been our capability of generating intense and continuous supersonic beams of oxygen atoms containing $O(^3P)$ and a small percentage of $O(^1D)$.[20] We have carried out experiments at two different collision energies (E_c), 13.4 and 15.5 kcal/mol. Under our experimental conditions we have been able to observe only the IO product (the major reaction pathway[18]) from the reactions:

$$O(^3P) + CH_3I \rightarrow IO + CH_3 \qquad \Delta H^\circ_0 = -0.7\pm2.0 \text{ kcal/mol} \quad (a)$$

$$O(^1D) + CH_3I \rightarrow IO + CH_3 \qquad \Delta H^\circ_0 = -46.3\pm2.0 \text{ kcal/mol} \quad (b)$$

The natural abundance of ^{13}C in the CH_3I beam produces a strong interference at the mass of the IO product, making the detection of IO difficult due to elastically scattered

$^{13}CH_3I$ contamination; therefore, to overcome this complication (which is severe at angles close to the CH_3I beam), we used isotopically labeled $^{18}O_2$ as precursor of atomic oxygen and detected the IO product at m/e=145. Product detection for reaction channels (1b) and (1c) are strongly kinematically unfavored, while product detection for channels (1d) and (1e) are hindered by the dissociative ionization in the ionizer of elastically scattered CH_3I.

From IO product angular and velocity distributions[21] (see Figs. 6-8), the dynamics of the reactions (a) and (b) were characterized. While IO coming from the $O(^1D)$ reaction arises from the decomposition of a long-lived complex (the dynamics is similar to that recently found[22] for the related reaction $O(^1D)+HI\rightarrow IO+H$), IO from the $O(^3P)$ reaction is found to be formed by two competing micro-mechanisms : direct reaction over the triplet PES giving backward scattered IO, and ISC from the triplet to the singlet PES with formation of a bound CH_3IO intermediate, which decomposes similarly to the $O(^1D)$ adduct, giving a backward-forward symmetric IO angular distribution in the c.m. frame. The best-fit c.m. angular and translational energy distributions at E_c=13.2 kcal/mol are shown in Fig. 9. In Figs. 6-8 the singlet and the two triplet contributions to the best-fit lab angular distributions are shown.

The resulting weight of the $O(^1D)$ contribution to the total c.m. function is ~35% of that of $O(^3P)$; this finding is not surprising, since the oxygen beam largely consists of $O(^3P)$, but the rate constant of $O(^1D)$, which is not known but can be estimated from the two values relative to the analogous reactions $O(^1D)+CH_3Cl$ and $O(^1D)+CH_3Br$, should be about one order of magnitude larger.

The fractions of reactive encounters which undergo ISC is found to be about 98% of the total $O(^3P)$ reactive collisions. ISC has been suggested by Grice et al.[23] to occur, but in smaller percentage, in the related $O(^3P)+RI$ reactions ($R=C_2H_5,(CH_3)_2CH$, $(CH_3)_3C$, CF_3CH_2, and CF_3) and has been correlated with the effect of charge transfer interaction on Renner Teller splitting of the triplet energy surface. Recent *ab initio* calculations on the singlet and triplet PES of the $O(^3P,^1D)+CH_3I$ system support the role of ISC for bent geometry.[24] Our results indicate that ISC is the dominant pathway, while the abstraction mechanism accounts for only a few percent of the total $O(^3P)$ reaction to form IO. The fact that the latter micro-mechanism is characterized by a sharply backward peaked angular distribution (see Figs. 6, 7 and 9) suggests that only for strictly collinear O-I-CH_3 geometry, within a narrow cone of acceptance, the reaction can proceed directly by abstraction on the triplet PES. The direct abstraction contribution is found to increase slightly as the collision energy is raised to 15.5 kcal/mol. In this respect, the dynamics of $O(^3P)+CH_3I\rightarrow IO+CH_3$ appears to be very different from the dynamics of the related reactions $O(^3P)+CF_3I\rightarrow IO+CF_3$ and $F(^2P)+CH_3I\rightarrow IF+CH_3$, where only the complex formation mechanism was observed to occur.[25] It would be interesting to have reliable triplet and singlet PES for the system and to carry out QCT calculations with surface hopping to simulate the experimental results and learn more about the role of electronically non adiabatic effects in oxygen atom reactions.

Magnetic analysis of supersonic beams of O, N and Cl atoms

We have produced supersonic beams of O, N, and Cl atoms and of metastable N_2 and O_2 molecules in our high-pressure radio-frequency discharge beam source and have characterized them by coupling velocity selection with magnetic analysis in the transmission mode.[26] The novelty of generating supersonic beams of N atoms of sufficient intensity to carry out crossed beam reactive scattering experiments was underlined in the 2nd year report and is exemplified in this report. The results, which are described in detail in ref. 26, can be summarized as follows.

We have found that oxygen atoms are produced mainly in the electronic ground state ^3P_J and a substantial relaxation within the fine level structure occurs during the supersonic expansion. An upper limit of 10% is derived for the relative concentration of atoms in the first electronically excited ^1D state in the beam.

In the case of N atoms, not only the ground electronic state ^4S, but also the metastable ^2D and ^2P states are formed in the discharge plasma ; in addition, the relaxation processes are ineffective and atoms in the beams have a high concentration of metastable states (^4S : 72%, ^2D : 21%, ^2P : 7%) (see Fig. 10). Since O(1D) and N(2D) atoms are metastable, they will survive up to the interaction region, and this allows us to study their reaction dynamics in crossed molecular beam experiments.

Cl atoms are produced exclusively in the ground electronic ^2P_J state (J=3/2,1/2), since excited electronic states are energetically inaccessible at the plasma temperatures. Atoms in the excited fine level $^2P_{1/2}$ are produced in high concentration (about 15-20%) in the discharge and scarcely relax during the supersonic expansion.

We have shown that an estimate of the relative population of electronic states in the beam on the basis of plasma temperatures or final translational temperatures can led to incorrect conclusions.

Finally, magnetic analysis has also been used to estimate the concentration of molecular oxygen in the first electronically excited $a^1\Delta_g$ state, which lies ≈1 eV above the ground state and has a lifetime of ≈44 minutes and can be present in the beam either because of incomplete dissociation or because of atomic recombination. A lower and upper limit of 15% and 40%, respectively, for the concentration of $O_2(a^1\Delta_g)$ in the beam was derived (see Fig. 11). Metastable $N_2(A\ ^3\Sigma_u^+)$ and $N_2(A'\ ^5\Sigma_u^+)$, which have an energy of 6.3 eV and ≈9.8 eV respectively over the ground state, have also been found to be present in the N beams.

NH beam generation

Test experiments have been carried out to ascertain the most efficient way to generate a supersonic beam of NH radicals. Unfortunately, RF discharge in dilute (about 2.5%) mixtures of NH_3 in He did not lead to NH beams of sufficient intensity to allow the study of the reaction :

$$NH + NO \rightarrow NNO + H \qquad \Delta H^\circ_0 = -34.7 \text{ kcal/mol}$$

The goal was to generate a beam of ^{15}NH to study the isotopic variant reaction

$$^{15}NH + NO \rightarrow {}^{15}NNO + H$$

by detecting N_2O at a mass-to-charge ratio *m/e*=45, for which our mass spectrometric detector has an inherent background of a factor about 20 lower than for *m/e*=44, but due to shortage of $^{15}N_2$ extensive tests were precluded. Of course, these attempts will continue in the next future. In particular, we think that a discharge in dilute N_2/H_2 mixtures in He (here, NH would originate from the reaction $N(^2D)+H_2$) may be more efficient, but, again, shortage of $^{15}N_2$ precluded the pursuit of this investigation for the moment. The effort was therefore concentrated towards the completion of the studies of $N(^2D)$ reactions already undertaken.

$N(^2D) + H_2$

The reaction of ground state atomic nitrogen $N(^4S)$ with molecular hydrogen is considerably endoergic (ΔH=21.7 kcal/mol), while that of electronically excited $N(^2D)$ is strongly exoergic:

$$N(^2D) + H_2 \rightarrow NH(v') + H \qquad \Delta H^\circ_0 = -33.2 \text{ kcal/mol}$$

and may lead to vibrationally excited imidogen radicals, in analogy to the corresponding $O(^1D) + H_2 \rightarrow OH(v') + H$ reaction. The room temperature rate constant for the reaction is reported to be about $5x10^{-12}$ cm^3 $molec^{-1}s^{-1}$.[27] (the reaction of $N(^2P)$ is known to be about two order of magnitude slower[27] than that of $N(^2D)$).

We had investigated the (technically easier) isotopic variant:

$$^{15}N(^2D) + D_2 \rightarrow {}^{15}ND(v') + D$$

at a collision energy of 5.1 kcal/mol (see 2nd year report). At this energy the ND radical can be populated up to v'=6 on energetic grounds. The angular and TOF data could be fitted with a symmetric c.m. angular distribution and using a translational energy distribution reflecting about 30% of the available energy released as product recoil energy. This indicates that the ND product should be highly internally excited. It was inferred that the reaction proceeds through insertion of $N(^2D)$ into the D-D bond to form a very short-lived NH_2 radical (amidogen) which dissociates rapidly after a few bending vibration, analogously to the formation of highly excited OD coming from the $O(^1D)+D_2$ reaction through a short lived H_2O intermediate.

During the past year, we have carried out new angular and velocity distribution measurements at a lower collision energy of E_c=3.8 kcal/mol to complement the data previously taken at E_c=5.1 kcal/mol (see Figs. 12 and 13). It is found that also at this lower E_c the NH product is formed strongly internally excited (about 30% of the total available energy is found to be channeled in translation), consistently with the results of recent spectroscopic investigation of this reaction by Umemoto and coworkers.[28] The c.m. angular distributions at E_c=3.8 kcal/mol (see Fig. 14) and 5.1 kcal/mol are backward-forward symmetric and reflect an insertion dynamics presumably via the ground state PES correlating with the ground state 1^2B_1 of NH_2. The absence of a preferential backward scattering with respect to the similar reaction $O(^1D)+D_2$ at E_c=5.3

kcal/mol[13] suggests that a direct abstraction mechanism does not occur, at least in this energy range.

Theoretical calculations of the experimental observables are being performed using the quasiclassical trajectory method by Schatz and coworkers[29] on a new *ab initio* PES calculated by Harding, Schatz and Rabitz.[30] Fig. 15 shows the schematic energy level and correlation diagram for the reaction $N(^2D) + H_2 \rightarrow NH + H$ according to the new accurate *ab initio* calculations of the PESs.[30] The insertion pathway on the ground state surface leading to the 1^2B_1 state of NH_2 is found[30] to have a barrier of about 1.7 kcal/mol in C_{2v} geometry and of about 4.7 kcal/mol for collinear approach ($C_{\infty v}$ geometry). These values can be contrasted with corresponding values of 0 and 0.7 kcal/mol, respectively, for the ground state PES of $O(^1D)+H_2$.[7,12] The first two excited PES $^2A_1$ and $^2B_2$ do not correlate with ground state $NH(X^3\Sigma^-)$, but with $NH(a^1\Delta)$ and $NH(b^1\Sigma^+)$, respectively, so neither can contribute adiabatically to the formation of ground state NH+H. For collinear approach the first excited PES $^2\Delta$ has a large barrier (> 20 kcal/mol) and does not correlate with ground state NH, which is quite different to what happens in the related $O(^1D)+H_2$ reaction, where the first excited PES $^1\Pi$ (in collinear geometry) has a barrier of 2.4 kcal/mol and correlates with ground state OH. These theoretical calculations suggest that only insertion plays a role in $N(^2D)+H_2$ at thermal energies, in contrast to $O(^1D)+H_2$. The $O(^1D)+H_2$ and $N(^2D)+H_2$ systems, indeed, although share a lot of similarities (see Fig. 16), do exhibit considerable differences in the topology of the PES (see Fig. 3 and 15). The absence of a backward scattered contribution in the angular distribution of $N(^2D)+D_2$ with respect to $O(^1D)+D_2$ can be even appreciated directly in the laboratory angular distribution data (see Fig. 17) : a clear indication that abstraction does not play a role in $N(^2D)+D_2$. The study of the various surfaces involved in this reaction, currently in progress in Schatz's group,[30] is showing a rather complex coupling scheme between the ground state PES and the first two excited PES, which could lead to a significant contribution to reaction via the excited state surfaces even at fairly low collision energies. In fact, insertion can come not only from the ground state PES, but also from the $^2A_1$ PES which is adiabatically connected to the $^2B_2$ state via non-C_{2v} geometry (a conical intersection exists between $^2A_1$ and $^2B_2$ surfaces) and the $^2B_2$ surface has a modest barrier of only 2.7 kcal/mol (for C_{2v} geometry) followed by a fairly deep well (see Fig. 15).

QCT calculations were performed by Schatz et al.[29,31] at the collision energies of the experiments on the ground state PES and calculated product angular and translational energy distribution were compared with the experimentally derived quantities. Quite good agreement is found for the angular distributions as can be seen in Fig. 14 for $N(^2D)+D_2$ at E_c=3.8 kcal/mol and very good accord exists for the translational energy distributions.[29, 31] Under our experimental conditions ND can only be formed in the ground state, but raising the collision energy sufficiently also allows for formation of $ND(a^1\Delta)$ (see Fig. 15): this will be explored in future experiments together with calculations of the excited $^2A_1$ PES correlating with $ND(a^1\Delta)$ which are currently in progress.

Recently, the dynamics of the $N(^2D)+H_2$ reaction has also been studied by QCT methods on a previous *ab initio* PES[32], and the results are quite different (backward scattered) since the abstraction barrier on this surface is lower than the insertion barrier. Very recently,[33] this surface has been modified to make the insertion barrier lower, and

the new results are very similar to what obtained on the new PES.[31] Dynamical calculations on this system have been carried out by quantum scattering methods (QM) for total angular momentum J=0 using several of the available potential energy surfaces, including the new one discussed here. The results are generally quite similar to the QCT results, indicating that the QCT results should be accurate.

A common feature to the $N(^2D)+H_2$ and $O(^1D)+D_2$ reactions is that the radical product is highly vibrationally excited, that is, infrared active. Therefore, both OH and NH emission in the infrared will occur in an environment where $O(^1D)$ and $N(^2D)$ are formed in the presence of H_2, as it can occur in the local atmosphere of the orbiting Space Shuttle.

$N(^2D) + C_2H_2$

In the 2nd year report the results of our crossed beam investigation of the reaction

$$N(^2D) + C_2H_2 \rightarrow HCCN + H \qquad \Delta H°_0 = -55 \text{ kcal/mol}$$

were described. Formation of the HCCN radical from this reaction has been suggested to be the first step in the formation of cyanogen, dicyanogen, HCN, etc. in the atmosphere of Titan.[34] The HCCN radical has also been observed in interstellar space[35] and has attracted much experimental and theoretical attention over the years.[36] Fig. 18 depicts a schematic energy level and correlation diagram for the $N(^4S, ^2D, ^2P) + C_2H_2$ system.

From product angular and velocity distributions at m/e=38 and 39, which were found to be identical, we concluded that HCCN formation was the observed reaction product, while the slightly more exoergic channel leading to CCN + H_2 does not occur appreciably. The HCCN lab angular and time-of-flight distributions at E_c=9.5 kcal/mol are shown in Fig. 19 and 20, respectively. The continuous lines represent the best-fit using a separable form of the center-of-mass frame product flux distribution, $I_{c.m.}(\vartheta, E)=T(\vartheta)P(E)$. The c.m. angular distribution was found to be symmetric at E_c=3.1 kcal/mol and somewhat forward peaked at the higher E_c of 9.5 kcal/mol. From this it was deduced that the reaction proceeds through a long-lived complex intermediate (presumably the cyanomethyl radical H_2CCN) at low E_c and through an osculating complex (i.e. a complex having a lifetime comparable to its rotational period) at the higher E_c.[37,38] The cyanomethyl radical is known to have a stability of about 110 kcal/mol with respect to dissociation into HCCN + H.[39] The fraction of total available energy released as product translational energy is 0.26 at both E_c. The remaining energy will be partitioned among the vibrational, rotational as well as electronic degrees of freedom of the HCCN radical (the singlet-triplet splitting of cyanomethylene is calculated to be 11.7 kca/mol).[40] The negligible polarization of the c.m. angular distribution reflects a high product rotational excitation.

Very recently, Takayanagi and coworkers[41] have carried out high-quality electronic structure calculations on the geometry and energy of the possible reaction intermediates and products of the $N(^2D)+C_2H_2$ reaction. Their work corroborates our finding and in particular shows that $N(^2D)$ attacks the two C-atoms of acetylene forming a cyclic intermediate which can lead to the very stable CH_2CN intermediate radical

complex by (1,2) H-shift and ring opening, or to a somewhat less stable linear HNCCH intermediate by simple ring opening. The internally hot complex will then dissociate under the single collision conditions of our experiment to HCCN + H by C-H or C-N bond cleavage.

In conclusion, the reaction of $N(^2D)$ with C_2H_2 produces HCCN radicals which are highly internally excited and, therefore, that may be optically active.

A detailed publication is in preparation.[38]

$N(^2D) + C_2H_4$

The reaction of $N(^4S)$ with C_2H_4 is known to be very slow ($K_{298}=10^{-16}$ cc molec^{-1} s^{-1}).[42] Using beams of $N(^4S,^2D)$, we have investigated the reaction with C_2H_4 at a collision energy of 7.95 kcal/mol and detected products only at m/e=40 (see Fig. 21). This is believed to originate from the reaction $N(^2D)+C_2H_4$ and to correspond to the H-displacement channel leading to the formation of CH_3CN (acetonitrile) ($\Delta H°_0$= – 107 kcal/mol) (or CH_2CHN), which fragments completely in the ionizer to give CH_2CN^+ (m/e=40). Data analysis in terms of an uncoupled center-of-mass angular distribution and translational energy distribution gives an average fraction of total available energy released in translation of 0.23, which indicates that the cyano-product being formed is highly internally excited. The c.m. angular distribution shows a broad forward peaking which suggests the intermediacy of an osculating complex. Noteworthy, acetonitrile has been recently observed in the atmosphere of Titan, where both $N(^2D)$ and C_2H_4 are present.[43]

The experimental data could also be fit assuming that molecular hydrogen elimination, leading to CH_2-CN (cyanomethyl) formation ($\Delta H°_0$= – 89 kcal/mol), takes place. However, the resulting fraction of energy channeled in translation would only be 13%, a rather modest (and perhaps unlikely) fraction. We think that formation of CH_2CN+H_2 is unlikely, since the three-four center elimination process which would be involved is expected to have a high energy barrier. Electronic structure calculations on the energetic of all possible intermediates and reaction products, as those recently carried out for $N(^2D)+C_2H_2$,[41] would be very valuable to assist the interpretation of the crossed beam data. These calculations may become available in the near future.

Second RF discharge source

The construction of a second radio-frequency discharge beam source, similar in characteristics to that described in ref. 20 and used in all the studies reported here, has been completed. The construction of a new set of RF electronics is at the final stage. This will allow us during the next future to attempt, by using the two RF discharges simultaneously, the dynamical study of radical-radical reactions as, for instance, N + OH $\rightarrow$NO + H.

CONCLUSIONS

From product angular and velocity distribution measurements in crossed beam experiments we have elucidated the dynamics of the following reactions :

1) $OH + CO \rightarrow CO_2 + H$
2) $OH + H_2 \rightarrow H_2O + H$
3) $O(^1D) + H_2 \rightarrow OH + H$
4) $O(^3P,^1D) + CH_3I \rightarrow IO + CH_3$
5) $N(^2D) + H_2 \rightarrow NH + H$
6) $N(^2D) + C_2H_2 \rightarrow HCCN + H$
7) $N(^2D) + C_2H_4 \rightarrow CH_3CN + H$

The experimental results have been compared, whenever possible, with state-of-the-art dynamical calculations (quasiclassical and/or quantum) on *ab initio* potential energy surfaces.

Reactions (1)-(3), and presumably also reactions (5) and (6), occur in the local atmosphere of the orbiting Space Shuttle. It has been shown that the products of some of these reactions, as the OH, NH, and HCCN radicals, and the H_2O molecule are formed highly vibrationally excited and therefore they will give rise to strong emission in the infrared. Furthermore, the subsequent reactivity of these reaction products will be considerably affected by their high internal energy content.

The information obtained from the study of these elementary reactions at the microscopic level, besides the interest from a fundamental point of view, is particularly relevant for a detailed understanding and modeling of the local atmosphere of the orbiting Space Shuttle. In particular, it may be useful for the improvement of the SOCRATES code, aimed at assessing the effects of contamination on measurements aboard spacecrafts in low Earth orbit. Ultimately, it should enable the world scientific community and the U.S. Air Force to better understand the local environment of space vehicles and of measuring platforms in space.

References

1. The OH product from the $O(^1D)+CH_4 \rightarrow OH+CH_3$ channel cannot be detected at m/e=17 using a beam of ^{16}O because of the interference from $^{13}CH_4$ (m/e=17) (present in the methane beam in natural abundance) elastically scattered from the oxygen beam. The use of a beam of ^{18}O was required, but unfortunately the detector background at m/e=19 was too large with respect to the reactive signal that a prohibitive amount of very expensive ^{18}O would have been required to gain a sufficient signal-to-noise ratio. (Using a beam of ^{16}O we were able to only look at the reaction channel $O(^1D)+CH_4 \rightarrow CH_3O+H$, but no significant improvement on the dynamics of this channel was obtained with respect to the previous study by P. Casavecchia, R.J. Buss, S.J. Sibener, and Y.T. Lee, J. Chem. Phys. 1980).
2. A.J. Alexander, F.J. Aoiz, M. Brouard, I. Burak, Y. Fujimura, J. Short, and J. P. Simons, Chem. Phys. Lett. **262**, 589 (1996) ; A.J. Alexander, F.J. Aoiz, M. Brouard, and J. P. Simons, Chem. Phys. Lett. **256**, 561 (1996) ; A.J. Alexander, D.A. Blunt, M. Brouard, J. P. Simons, F.J. Aoiz, L. Banares, Y. Fujimura, and M. Tsubouchi, Faraday Discuss. **108**, xxx (1997).
3. D.-C. Che and K. Liu, J. Chem. Phys. **103**, 5164 (1995) ; Y.-T. Hsu and K. Liu, J. Chem. Phys. **107**, 1664 (1997) ; Y.-T. Hsu, J.-H. Wang, and K. Liu, J. Chem. Phys. **107**, 2351 (1997).
4. R.K. Talukdar and A.R. Ravishankara, Chem. Phys. Lett. **253**, 177 (1996).
5. T. Laurent, P.D. Naik, H.-R. Volpp, J. Wolfrum, T. Arusi-Parpar, I. Bar, and S. Rosenwaks, Chem. Phys. Lett. **236**, 343 (1995); S. Koppe, T. Laurent, P.D. Naik, H.-R. Volpp, J. Wolfrum, T. Arusi-Parpar, I. Bar, and S. Rosenwaks, Chem. Phys. Lett. **214**, 546 (1993).
6. A.G. Suits, private communication
7. T.-S. Ho, T. Hollebeek, H. Rabitz, L.B. Harding, and G.C. Schatz, *J. Chem. Phys.* 1996, **105**, 10472; G.C. Schatz, A. Papaioannou, L.B. Harding, T.-S. Ho, T. Hollebeek, and H. Rabitz, *J.Chem. Phys.* 1997, **107**, 2340.
8. T. Peng, D.H. Zhang, J.Z.H. Zhang, and R. Schinke, Chem. Phys. Lett. **248**, 37 (1996).
9. J. Dai, J. Chem. Phys.**107**, 4934 (1997).
10. A.J.C. Varandas, J. Chem. Phys. **105**, 3524 (1996) ; A.J.C. Varandas, A.I. Vovonin, A. Riganelli, and P.J.S.B.Caridade, Chem. Phys. Lett. **278**, 325 (1997).
11. A. Dobbyin and P.J. Knowles, Mol. Phys. **91**, 1107 (1997).
12. G.C. Schatz, L.A. Pederson, and P.J. Kuntz, Faraday Discuss. **108**, xxx (1997).
13. M. Alagia, N. Balucani, L. Cartechini, P. Casavecchia, E.H. van Kleef, G.G. Volpi, P.J.Kuntz, and J.J. Sloan, *J. Chem. Phys.*(1998), in press.
14. R. Polák, K. Paiderová, and P.J. Kuntz, J. Chem. Phys., **87** 2863 (1987).
15. M. Alagia, N. Balucani, L. Cartechini, P. Casavecchia, E.H. van Kleef, G.G. Volpi, L. Harding, H. Rabitz, T. Hollebeek, T.-S. Ho, L.A. Pederson, and G.C. Schatz, Faraday Discuss. **108**, xxx (1997).

16. P.M. Aker and J.J. Sloan, J. Chem. Phys. **85**, 1412 (1986).

17. Solomon, S.; Garcia, R.R.; Ravishankara, A.R. *J. Geophys. Research* **1994**, *99(D10)*, 20491. See also (b) Solomon, S.; Burkholder, J.B.; Ravishankara, A.R.; Garcia, R.R. *J.Geophys. Research* **1994**, *99(D10)*, 20929.
18. Gilles, M.K.; Turnipseed, A.A.; Rudich, Y.; Talukdar, R.K.; Villalta, P.; Huey, L.G.; Burkholder, L.B.; Ravishankara, A.R. *J. Phys. Chem.* **1996**, *100*, 14005.
19. Thompson, J.E.; Ravishankara, A.R. *Int. J. Chem. Kin.* **1993**, *25*, 479; Force, A.P.; Wiesenfeld, J.R. *J. Phys. Chem.* **1981**, *85*, 782.
20. Casavecchia, P; Balucani., N; Volpi, G.G. In *Research in Chemical Kinetics*, Vol. 1; Compton, R.G.; Hancock, G., Eds.; Elsevier: Amsterdam, 1993; p.1. (b) Casavecchia, P; Balucani., N; Volpi, G.G. In *Advanced Series in Physical Chemistry - Vol.6. The Chemical Dynamics and Kinetics of Small Radicals*; Wagner, A.; Liu, K., Eds; Worlds Scientific: Singapore, 1995; p. 365. (c) Alagia, M.; Balucani, N.; Casavecchia, P.; Stranges, D.; Volpi, G.G. *J. Chem. Soc. Faraday Trans.* **1995**, *91*, 575.
21. Alagia, M.; Balucani, N., Cartechini, L., Casavecchia, P., van Beek, M., and Volpi, G.G., Faraday Discuss. **108**, xxx (1997) ; also, in preparation.
22. Alagia, M.; Balucani, N.; Casavecchia, P.; Volpi, G.G. *J. Phys. Chem. A* **101**, 6455 (1997).
23. Wang, J.J.; Smith, D.J.; Grice, R. *J.Phys.Chem.* **1996**, *100*, 6620; *ibidem* 13603.
24. Misra, A., Berry, R.J., and Marshall, P., J. Phys. Chem. A **101**,7420 (1997).
25. Farrar, J.M.; Lee, Y.T. *J. Chem. Phys.* **1975**, *63*, 3639. Buss, R.J.; Sibener, S.J.; Lee, Y.T. *J. Phys.Chem.* **1983**, *87*, 4840.
26. M. Alagia, V. Aquilanti, D. Ascenzi, N. Balucani, D. Cappelletti, L. Cartechini, P. Casavecchia, F. Pirani, G. Sanchini, and G.G. Volpi, *Israel J. Chem. (Issue on Molecular Beams) **36**, xxx (1997).*
27. T. Suzuki, Y. Shihira, T. Sato, H. Umemoto, and S. Tsunashima, *J. Chem. Soc. Faraday Trans.* 1993, **89**, 995.
28. H. Umemoto and K. Matsumoto, *J. Chem. Phys.* **104**, 9640 (1996); H. Umemoto, T.Asai, and Y. Kimura, *J. Chem. Phys.* 1997, **106**, 4985.
29. P. Casavecchia, M. Alagia, N. Balucani, L. Cartechini, G.G. Volpi, G.C. Schatz, L. Pederson, G. Lendway, L.R. Harding, T. Hollebeek, H. Rabitz, and T. Takayanagi, *Faraday Discussion **108**, xxx (1997).*
30 L. Harding, H. Rabitz, and G.C. Schatz, *work in progress.*
31. P. Casavecchia, M. Alagia, N. Balucani, L. Cartechini, G.G. Volpi, G.C. Schatz, L. Pederson, G. Lendway, L.R. Harding, T. Hollebeek, H. Rabitz, and T. Takayanagi, *in preparation.*
32. T.Takayanagi, H.Koboyashi, and S. Tsunashima, *J.Chem.Soc.Far.Trans.* 1996, **92**, 1311 ; H.Koboyashi, T.Takayanagi, K. Yokoyama, T. Sato, and S. Tsunashima, *J.Chem.Soc.Far.Trans.* 1996, **91**, 3771.
33. H.Koboyashi, T.Takayanagi, and S. Tsunashima, *Chem. Phys. Lett.* 1997, **277**, 20.
34. Y.L. Yung, Icarus **72**, 468 (1987).
35. S.E. Cummins, R.A. Linke, and P. Thaddeus, Astrophys. J. Suppl. **60**, 819 (1986).

36. M.C. McCarthy, C.A. Gottlieb, A.L. Cooksy, and P. Thaddeus, J. Chem. Phys. **103**, 7779 (1995), and references therein; N. Goldberg, A. Fiedler, and H. Schwarz, J. Phys. Chem. **99**, 15327 (1995), and references therein.
37. P. Casavecchia, M. Alagia, N. Balucani, L. Cartechini, and G.G. Volpi, *Faraday Discuss. **108**, xxx (1997).*
38. P. Casavecchia, M. Alagia, N. Balucani, L. Cartechini, and G.G. Volpi, *in preparation.*
39. S. Moran, H.B. Ellis, Jr., D.J. DeFrees, A.D. McLean, and G.B. Ellison, J. Am. Chem. Soc. **109**, 55996 (1987).
40. J.S. Francisco, Chem. Phys. Lett. **231**, 372 (1994).
41. T. Takayanagi, *private communication.*
42. J.V. Michael, Chem. Phys. Lett. **76**, 129 (1980).
43. B. Bezard, A. Marten, and G. Paubert, Bull. Am.Astron. Society **25**, 1100 (1993).

Figure Captions

Fig. 1. OH (OD) product laboratory angular distributions for the $O(^1D)+H_2$ reaction at E_c=0.88, 1.9 and 3.0 kcal/mol (top three panels) and $O(^1D)+D_2$ at E_c=5.3 kcal/mol (bottom panel). Solid lines : calculated curves with best fit center-of-mass angular and translational energy distributions. Dashed lines : QCT predictions on ground state DIM surface. Canonical Newton diagrams are also shown on the r.h.s.; there the circles delimit the maximum speed that the OH(OD) product can attain assuming that all the available energy is channeled into translation.

Fig. 2. Center-of-mass product angular distributions for the same reactions of Fig. 1. An increasing backward bias can be noted with increasing E_c.

Fig. 3. Schematic energy level and correlation diagram for $O(^1D)+H_2$.

Fig. 4. Comparison between the experimentally derived OD product angular distribution (solid line) from the $O(^1D)+D_2$ reaction at E_c=5.3 kcal/mol and QCT calculations (dashed lines) on the ground state $1^1A'$ and first excited state 1A" PES. The summed contribution ($1^1A'$ + 1A") is also shown.

Fig. 5. The singlet (solid line) and the triplet (dashed line) potential energy surfaces (schematic) for the reaction $O(^3P,^1D) + CH_3I \rightarrow IO + CH_3$ with intersystem crossing (ISC).

Fig. 6. Laboratory angular distribution (dots) of the IO product at E_c=15.3 kcal/mol from the reactions $O(^3P,^1D) + CH_3I \rightarrow IO + CH_3$ The circles in the velocity vector ("Newton") diagram delimit the maximum velocity that the IO product can attain on the basis of energy conservation if all the available energy for the triplet and the singlet reactions goes into product translational energy. The separate contributions to the total lab angular distribution (heavy solid line) from the singlet reaction (light solid line), the direct triplet reaction (short dashed line) and the triplet reaction via ISC (long dashed line) are shown.

Fig. 7. As in Fig. 6, but for E_c=13.2 kcal/mol.

Fig. 8. Time-of-flight (TOF) distributions of the IO product at E_c=13.2 kcal/mol. The separate contributions to the TOF spectra are shown (notation as in Fig. 6).

Fig. 9. Center-of-mass product angular and translational energy distributions at E_c=13.2 kcal/mol.

Fig. 10. Beam transmittance for the supersonic beam of ^{14}N seeded in Ne as a function of the magnetic field B at the indicated velocity. Dotted-dashed, dashed and long-dashed lines are calculated assuming the exclusive population of ^4S, ^2D and ^2P, respectively ; the best-fit calculation is reported as solid line and corresponds to a total concentration of the two metastable states equal to 28% (^4S : 72%, ^2D : 21%, ^2P : 7%).

Fig. 11. Beam transmittance I/I_0 for the O_2 beam seeded in Ne, measured as a function of magnetic field B at v=1210 m/s. The long-dashed line is the calculated I/I_0 for a pure $^3\Sigma_g^-$ state, while the dashed line refers to a pure $^1\Delta_g$ state, both calculations being performed assuming a rotational temperature T_r=600 K ; the solid line is the best fit calculation which gives the lower limit (~15%) of $^1\Delta_g$ concentration. Similar calculations assuming T_r=30 K give the upper limit ~40%.

Fig. 12 Lab angular distribution of the ND product from the $N(^2D)+D_2$ reaction at E_c=3.8 and 5.1 kcal/mol. Solid lines : calculations with best fit c.m. angular and translational energy distributions.

Fig. 13 TOF distributions of the ND product at selected lab angles for the two collision energies of Fig. 12.

Fig. 14 Best-fit c.m. ND angular distribution at E_c=3.8 kcal/mol compared with the results of QCT calculations by Schatz et al. on a new *ab initio* ground state NH_2 PES.

Fig. 15 Schematic (semi-quantitative) energy level and correlation diagram for the $N(^2D)+H_2$ reaction based on *ab initio* calculations of the ground and excited PES by Harding, Schatz, Rabitz and coworkers.

Fig. 16 Energy levels for the $O(^1D)+D_2$ and $N(^2D)+D_2$ reactions.

Fig. 17 Lab angular distribution of the OD product from the $O(^1D)+D_2$ reaction at E_c=5.3 kcal/mol (l.h.s.) compared to that of the ND product from the $N(^2D)+D_2$ reaction at E_c=5.1 kcal/mol (r.h.s.). The corresponding Newton diagrams are also shown underneath the angular distributions.

Fig. 18 Schematic energy level and correlation diagram for the $N(^4S, ^2D, ^2P) + C_2H_2$ system.

Fig. 19 Laboratory angular distribution of the HCCN product (detected at m/e=38) from the $N(^2D)+C_2H_2$ reaction at E_c=9.5 kcal/mol. The circle in the canonical Newton diagram delimits the maximum speed that the HCCN product can attain if all the available energy is channeled into translation.

Fig. 20 TOF distributions at selected lab angles of the HCCN product from the $N(^2D)+C_2H_2$ reaction at E_c=9.5 kcal/mol.

Fig. 21 Lab angular distribution and TOF spectra at selected angles of the CH_3CN product (detected at m/e=40) from the $N(^2D)+C_2H_4$ reaction at Ec=7.95 kcal/mol.

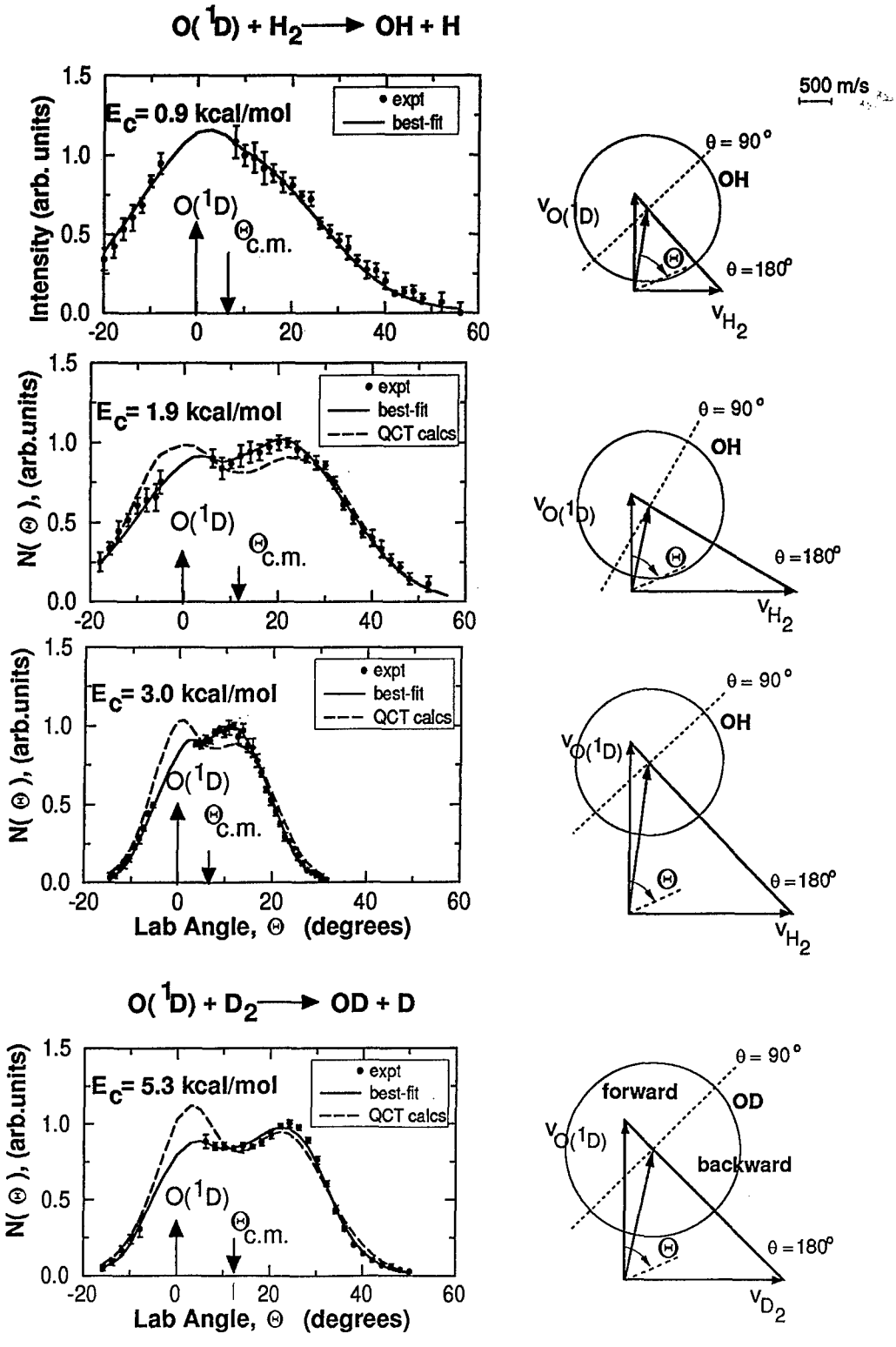
O(1D) + H2 → OH + H
500 m/s
Ec= 0.9 kcal/mol
• expt
best-fit
Intensity (arb. units)
O(1D)
Θc.m.
θ = 90°
OH
θ=180°
vO(1D)
vH2
Ec= 1.9 kcal/mol
• expt
best-fit
QCT calcs
N(Θ), (arb.units)
Ec= 3.0 kcal/mol
Lab Angle, Θ (degrees)
O(1D) + D2 → OD + D
Ec= 5.3 kcal/mol
forward
backward
OD
vD2

Fig. 1

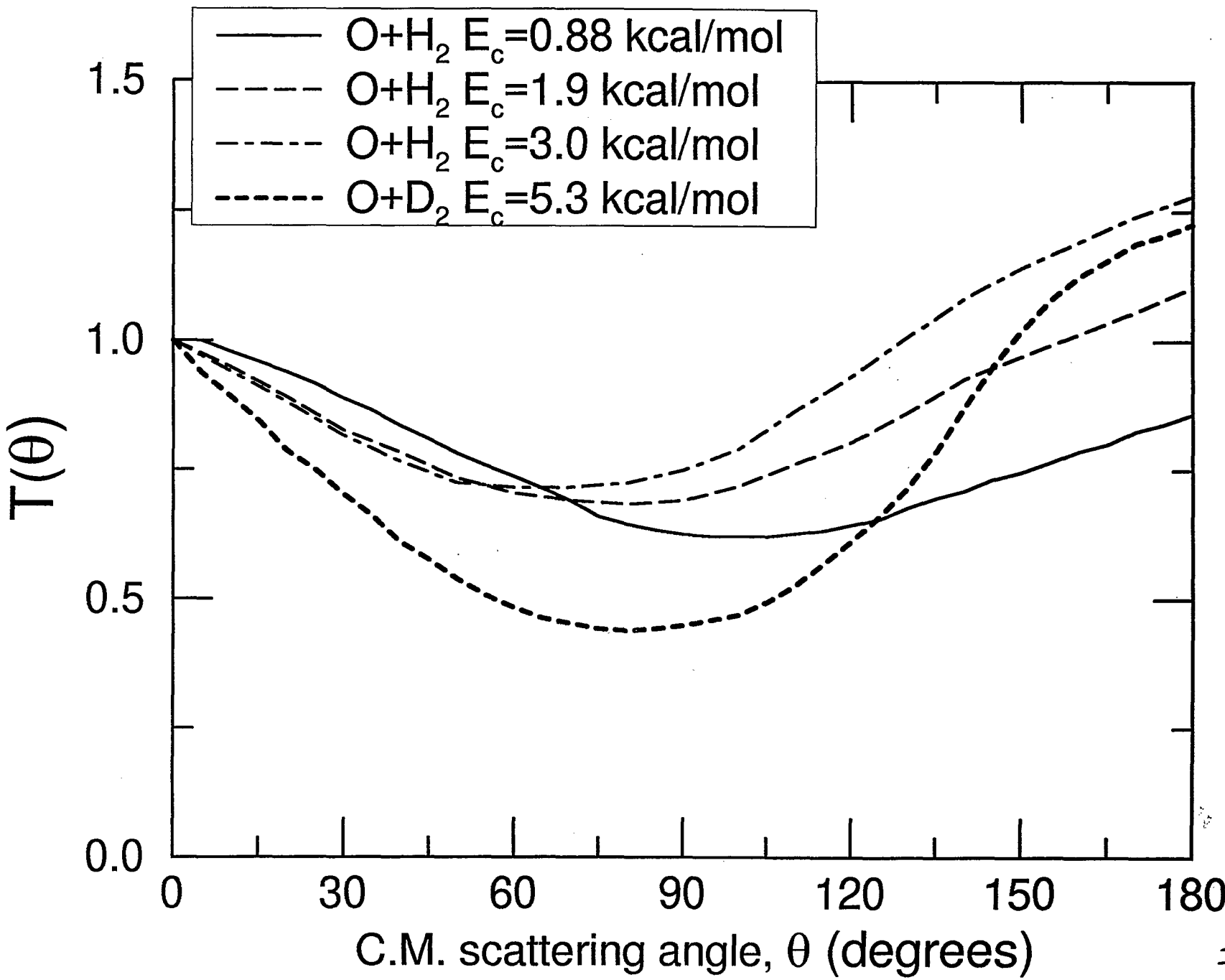
O+H2 Ec=0.88 kcal/mol
O+H2 Ec=1.9 kcal/mol
O+H2 Ec=3.0 kcal/mol
O+D2 Ec=5.3 kcal/mol
T(θ)
1.5
1.0
0.5
0.0
0
30
60
90
120
150
180
C.M. scattering angle, θ (degrees)

Fig. 2

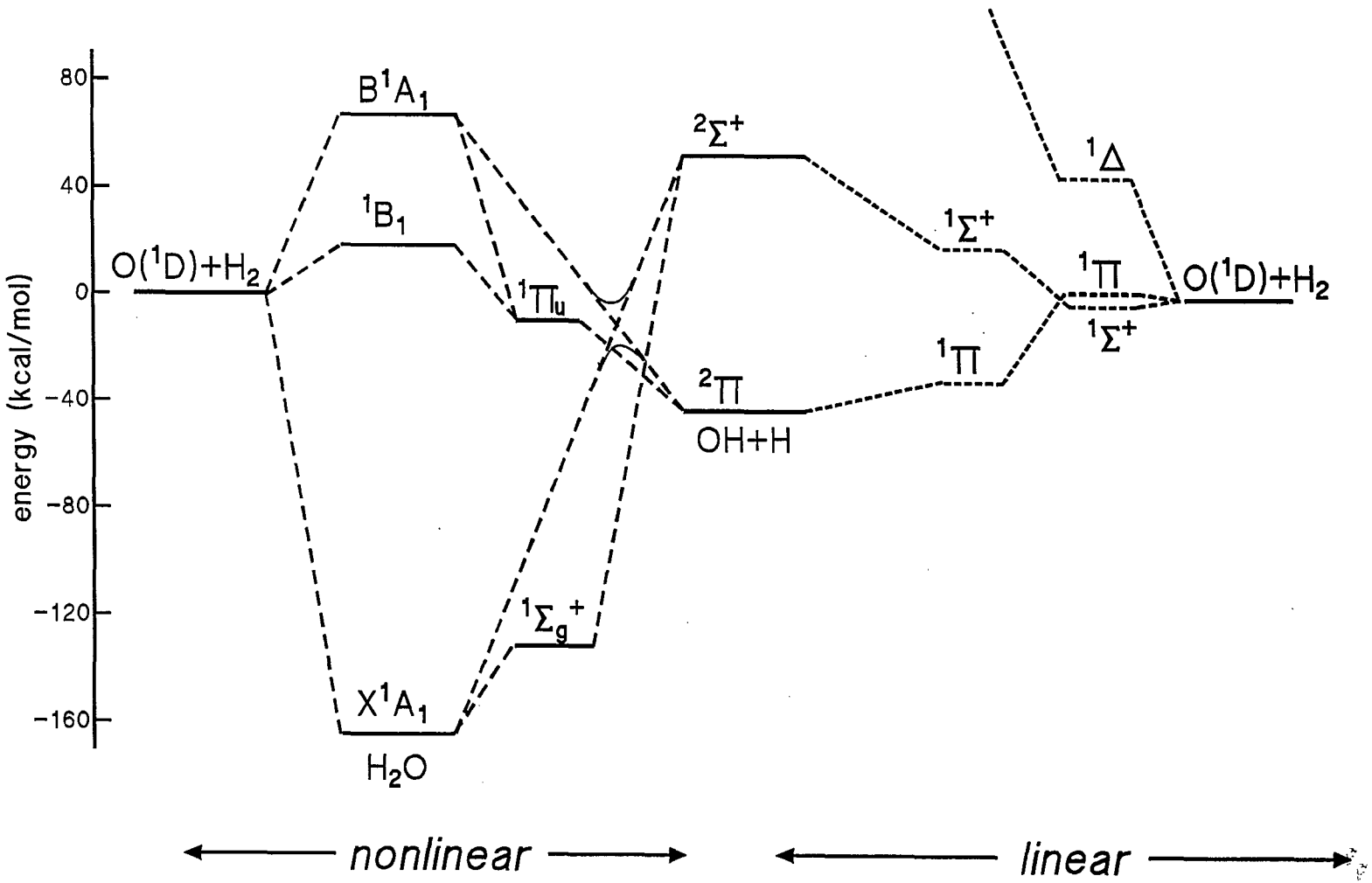
80
40
0
−40
−80
−120
−160
energy (kcal/mol)
B¹A₁
¹B₁
O(¹D)+H₂
¹Πu
²Σ⁺
¹Δ
¹Σ⁺
¹Π
O(¹D)+H₂
¹Σ⁺
¹Π
²Π
OH+H
¹Σg⁺
X¹A₁
H₂O
nonlinear
linear

Fig. 3

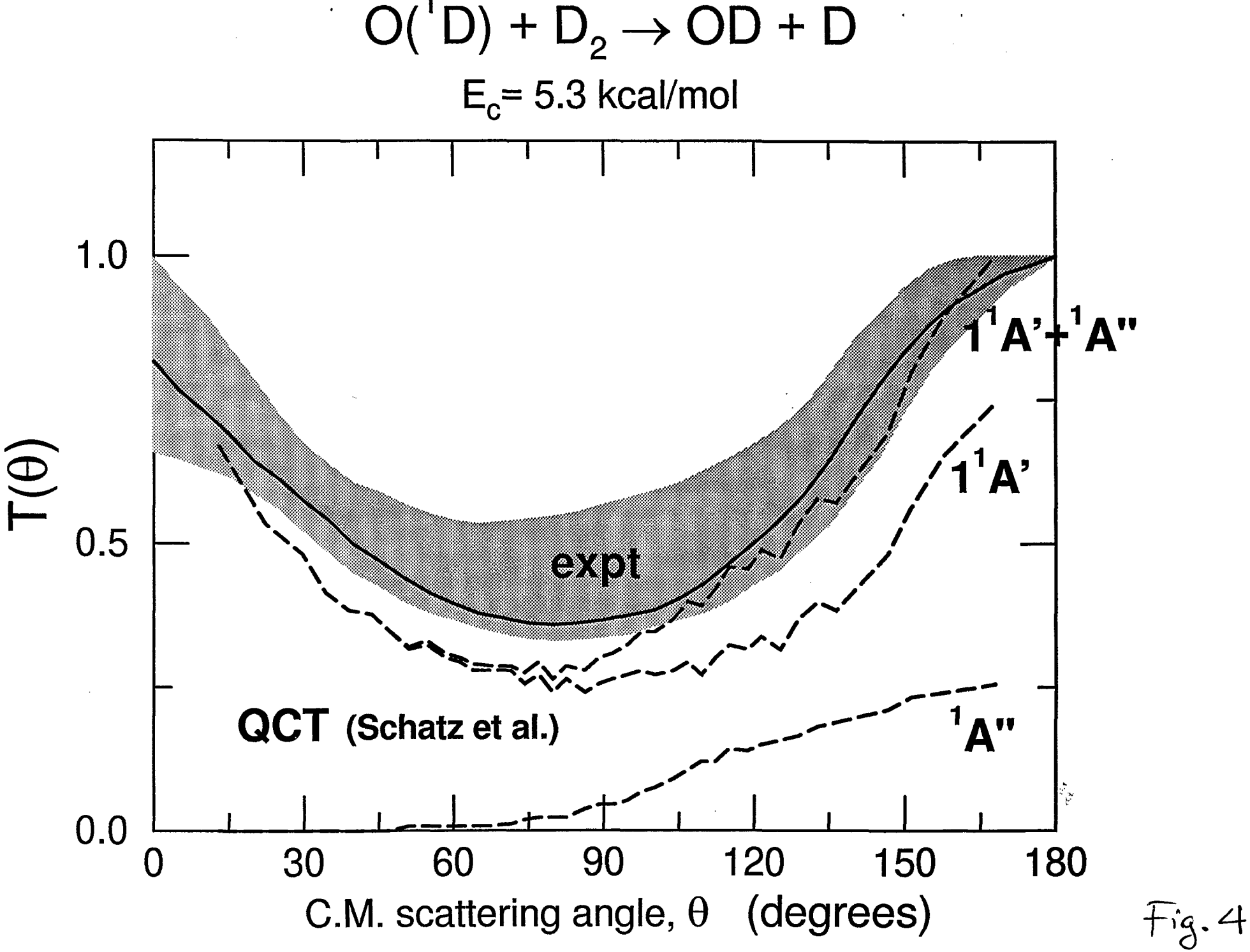
O(1D) + D2 → OD + D
Ec= 5.3 kcal/mol
T(θ)
1.0
0.5
0.0
0
30
60
90
120
150
180
C.M. scattering angle, θ (degrees)
expt
1 1A'+1A"
1 1A'
1A"
QCT (Schatz et al.)

Fig. 4

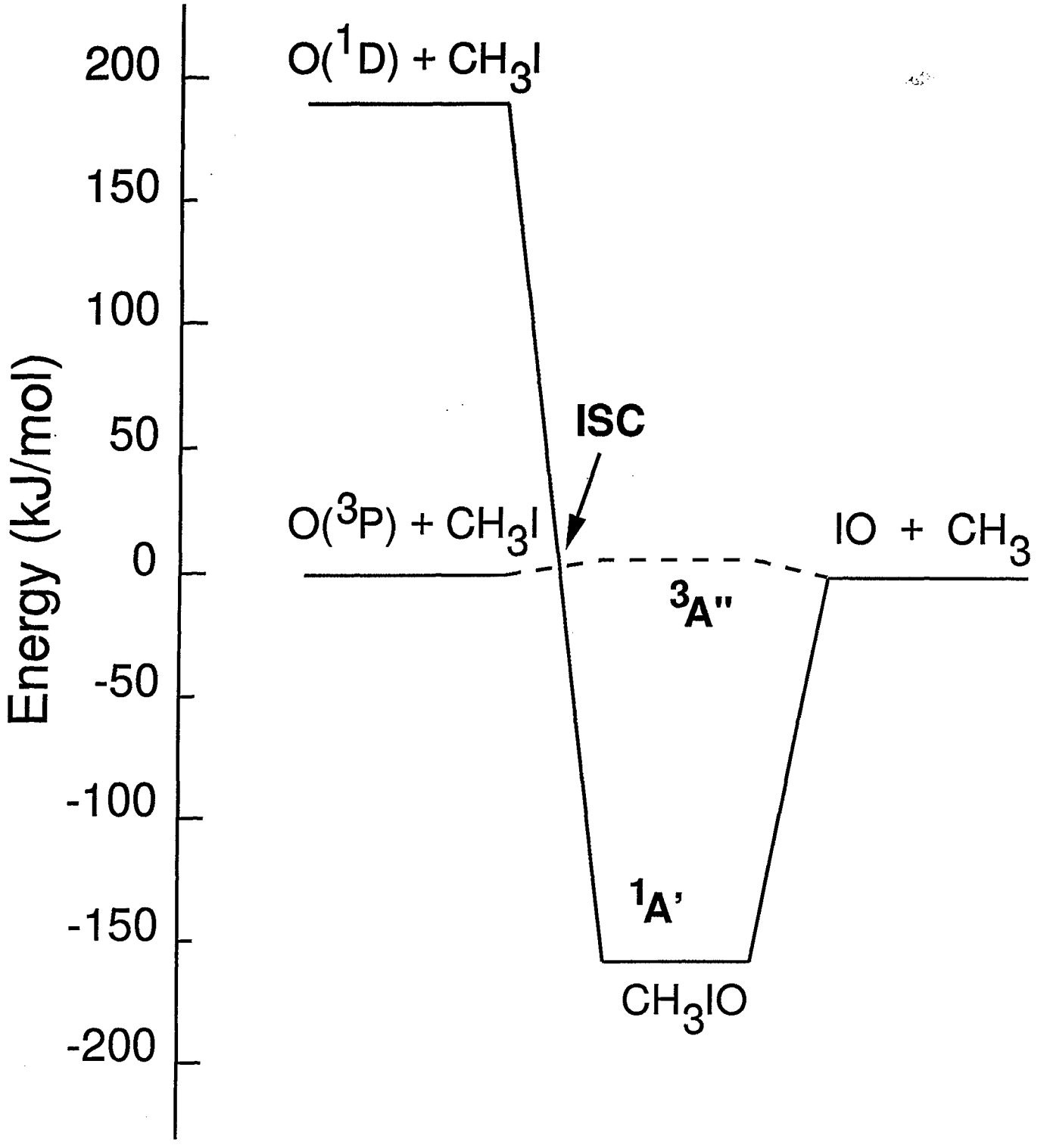
200
150
100
50
0
-50
-100
-150
-200
Energy (kJ/mol)
O(1D) + CH3I
ISC
O(3P) + CH3I
IO + CH3
3A"
1A'
CH3IO

Fig. 5

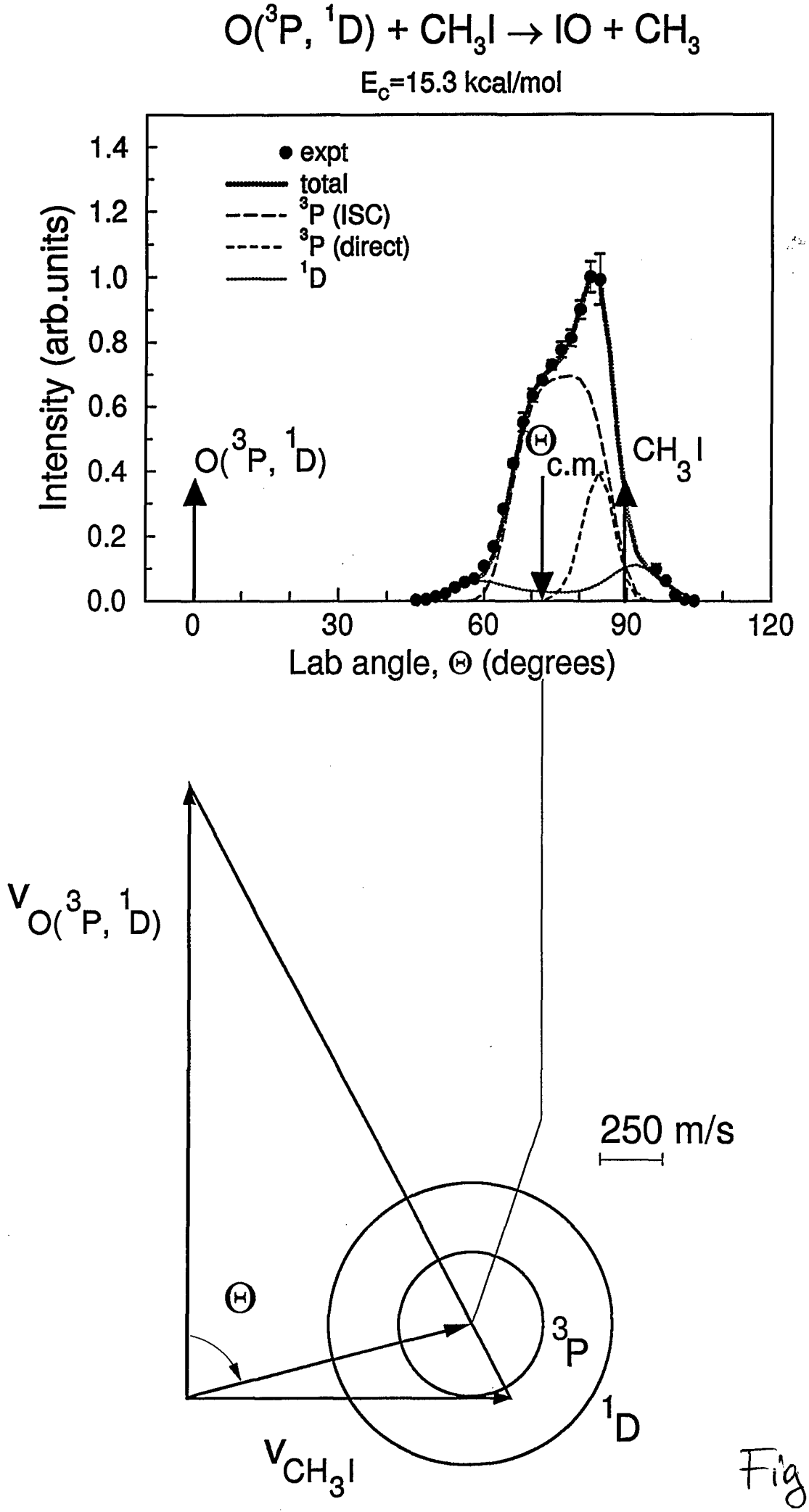
O(3P, 1D) + CH3I → IO + CH3
Ec=15.3 kcal/mol
expt
total
3P (ISC)
3P (direct)
1D
Intensity (arb.units)
1.4
1.2
1.0
0.8
0.6
0.4
0.2
0.0
O(3P, 1D)
Θc.m.
CH3I
0
30
60
90
120
Lab angle, Θ (degrees)
VO(3P, 1D)
250 m/s
Θ
3P
1D
VCH3I

Fig. 6

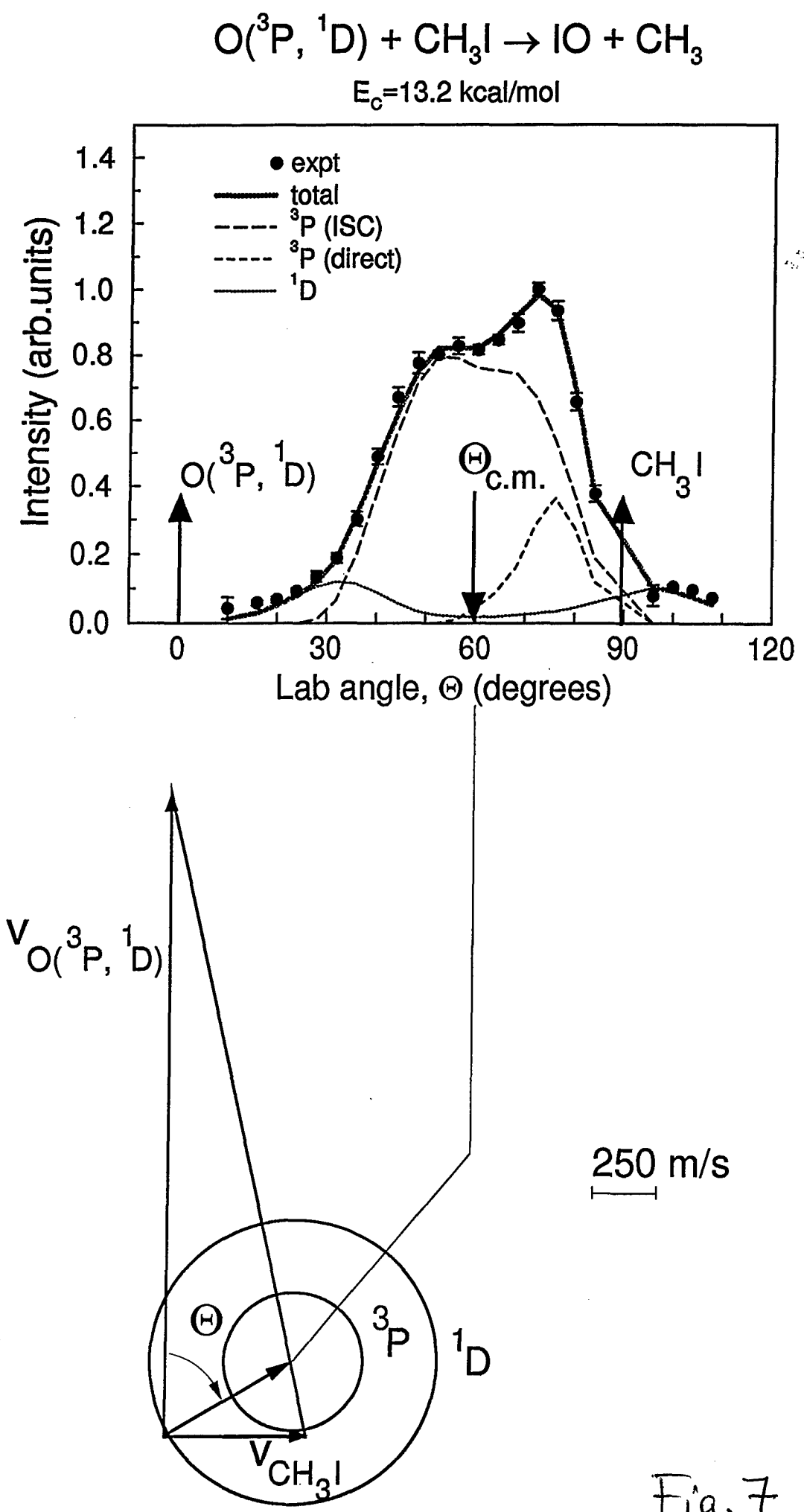
O(3P, 1D) + CH3I → IO + CH3
Ec=13.2 kcal/mol
expt
total
3P (ISC)
3P (direct)
1D
Intensity (arb.units)
1.4
1.2
1.0
0.8
0.6
0.4
0.2
0.0
O(3P, 1D)
Θc.m.
CH3I
0
30
60
90
120
Lab angle, Θ (degrees)
VO(3P, 1D)
250 m/s
Θ
3P
1D
VCH3I

Fig. 7

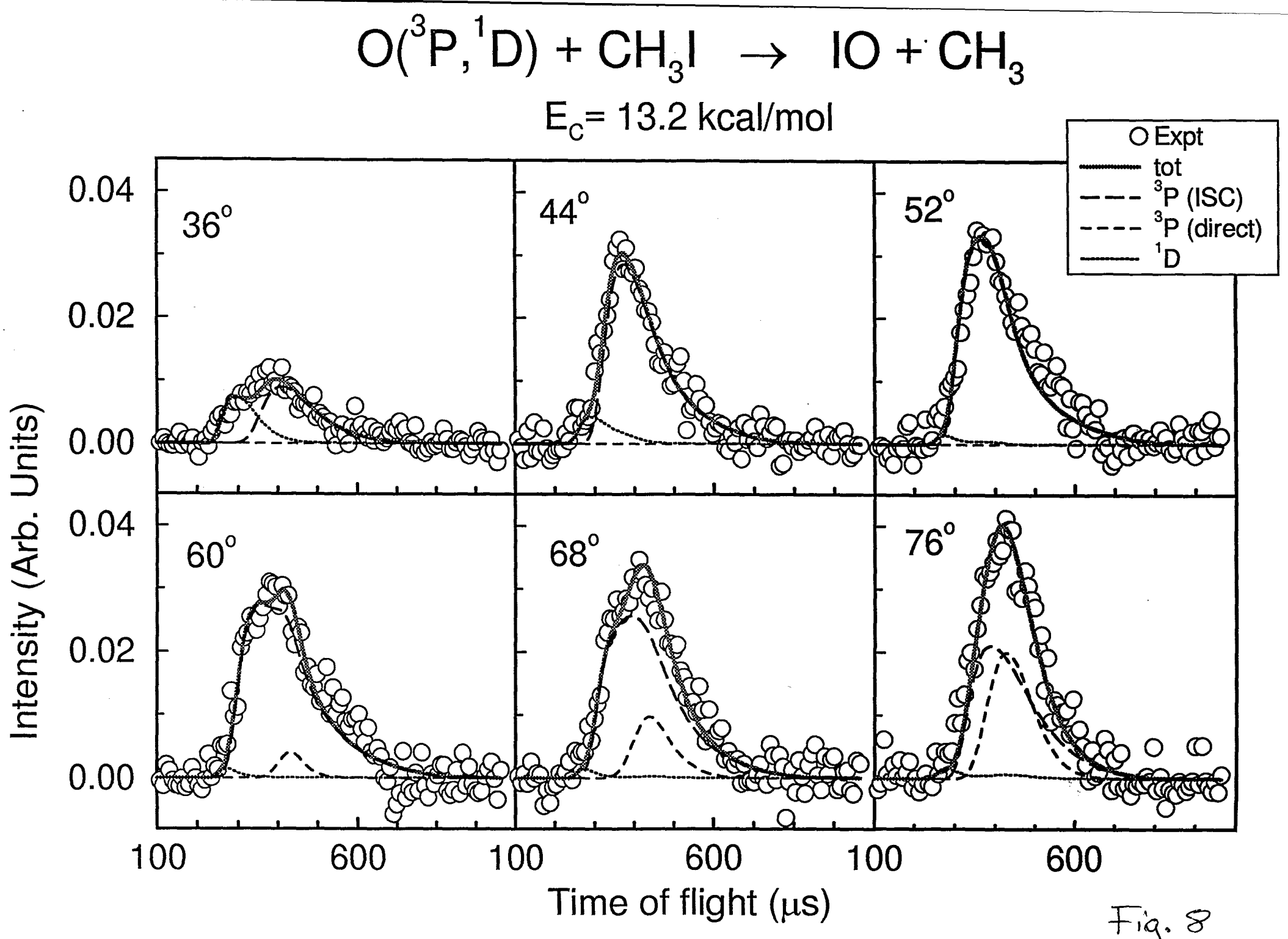
O(3P,1D) + CH3I → IO + CH3
Ec= 13.2 kcal/mol
O Expt
tot
3P (ISC)
3P (direct)
1D
36°
44°
52°
60°
68°
76°
0.04
0.02
0.00
Intensity (Arb. Units)
100
600
Time of flight (μs)

Fig. 8

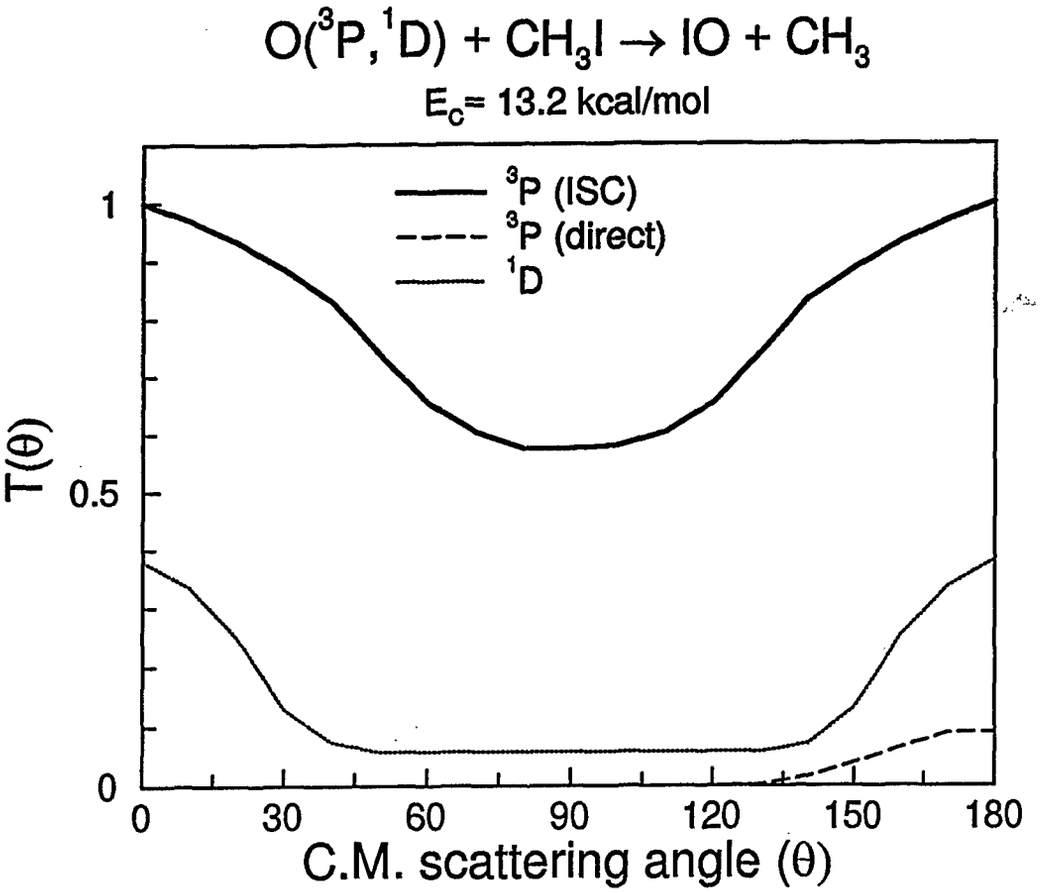
$O(^3P,^1D) + CH_3I \rightarrow IO + CH_3$
E_c= 13.2 kcal/mol
^3P (ISC)
^3P (direct)
^1D
T(θ)
1
0.5
0
0
30
60
90
120
150
180
C.M. scattering angle (θ)

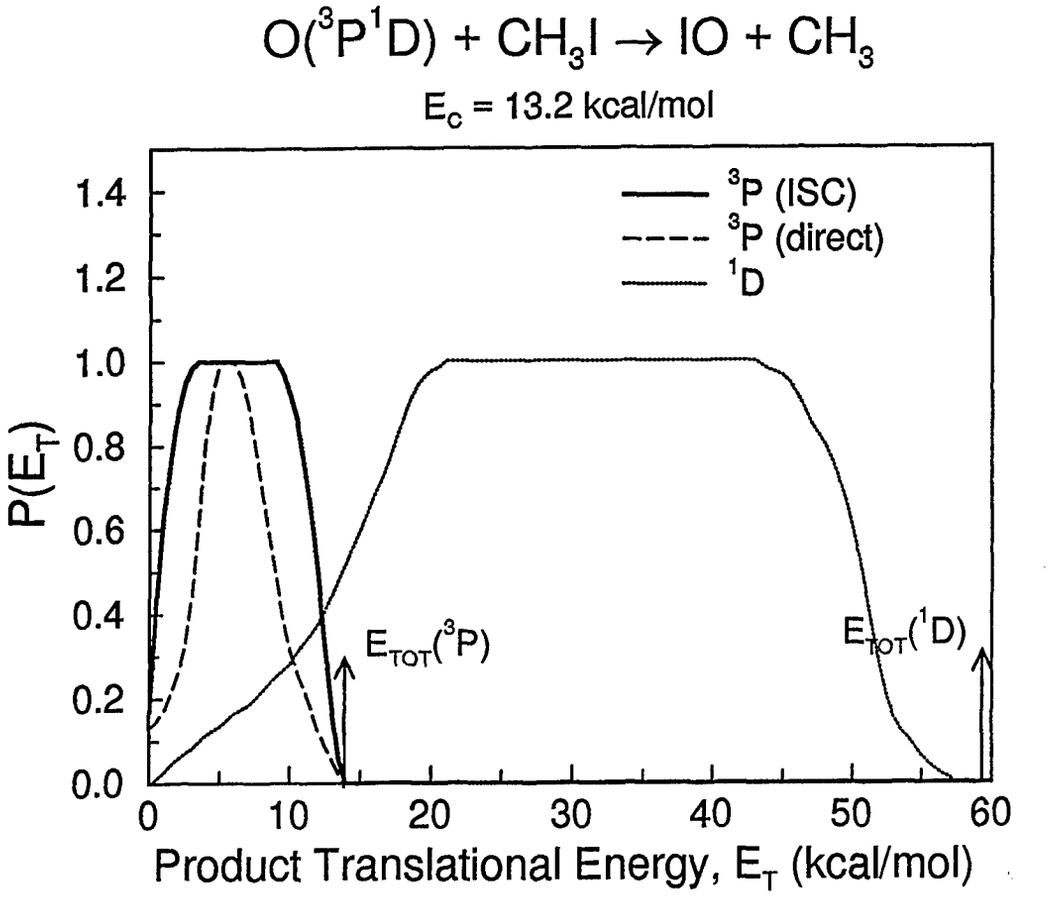
$O(^3P^1D) + CH_3I \rightarrow IO + CH_3$
E_c = 13.2 kcal/mol
^3P (ISC)
^3P (direct)
^1D
$P(E_T)$
1.4
1.2
1.0
0.8
0.6
0.4
0.2
0.0
$E_{TOT}(^3P)$
$E_{TOT}(^1D)$
0
10
20
30
40
50
60
Product Translational Energy, E_T (kcal/mol)

Fig. 9

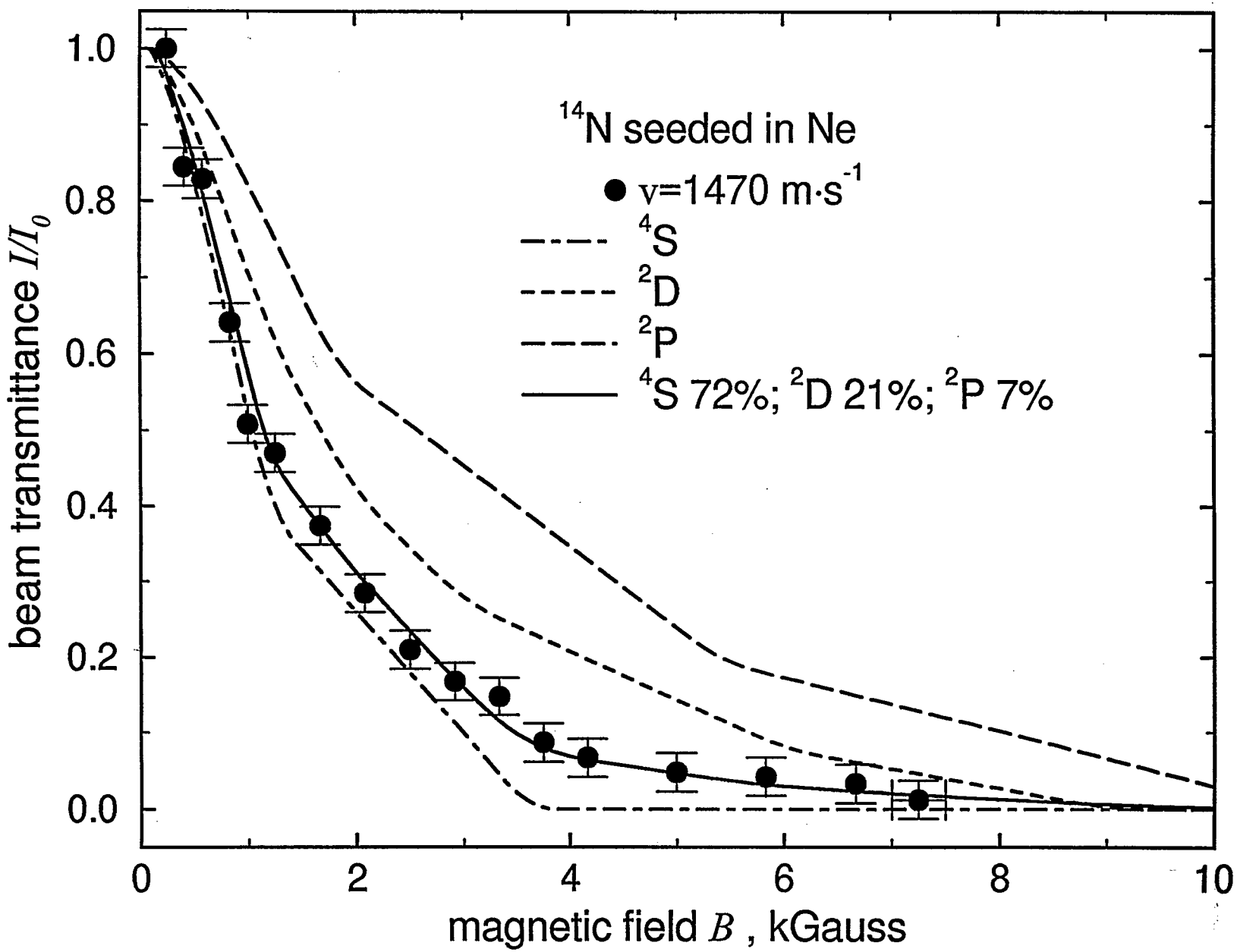
1.0
0.8
0.6
0.4
0.2
0.0
beam transmittance I/I_0
0
2
4
6
8
10
magnetic field B , kGauss
^{14}N seeded in Ne
v=1470 m·s^{-1}
^{4}S
^{2}D
^{2}P
^{4}S 72%; ^{2}D 21%; ^{2}P 7%

Fig. 10

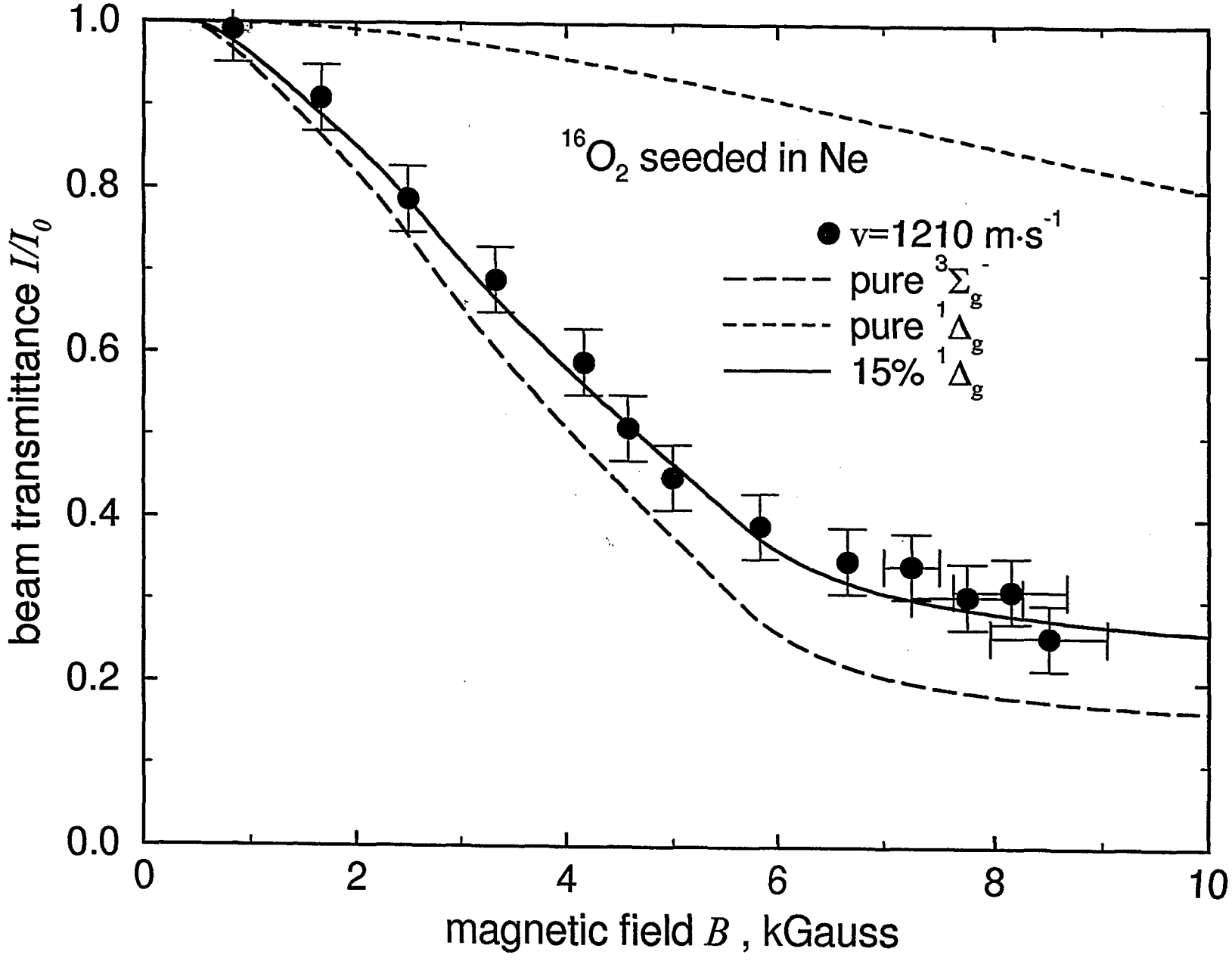
1.0
0.8
0.6
0.4
0.2
0.0
beam transmittance I/I_0
0
2
4
6
8
10
magnetic field B , kGauss
$^{16}O_2$ seeded in Ne
v=1210 m·s^{-1}
pure $^3\Sigma_g^-$
pure $^1\Delta_g$
15% $^1\Delta_g$

Fig. 11

$N(^2D) + D_2 \rightarrow ND + D$

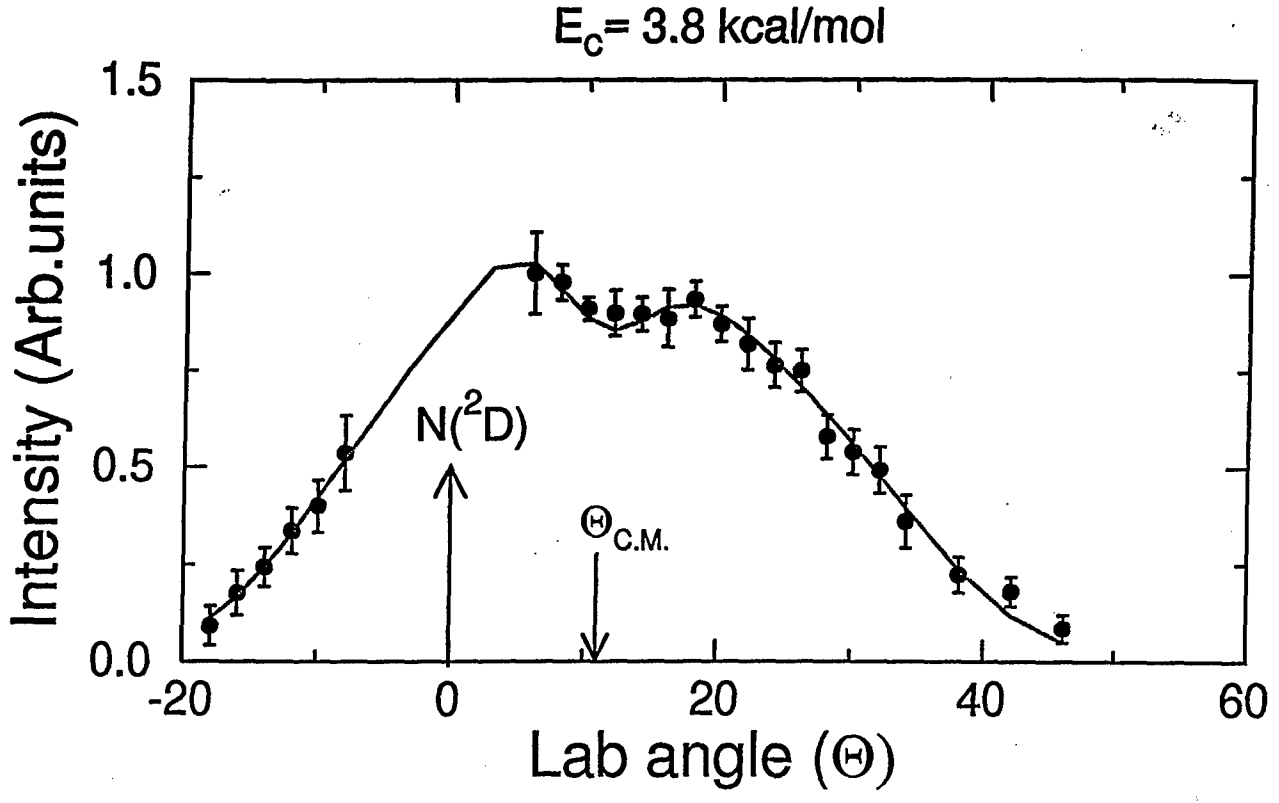

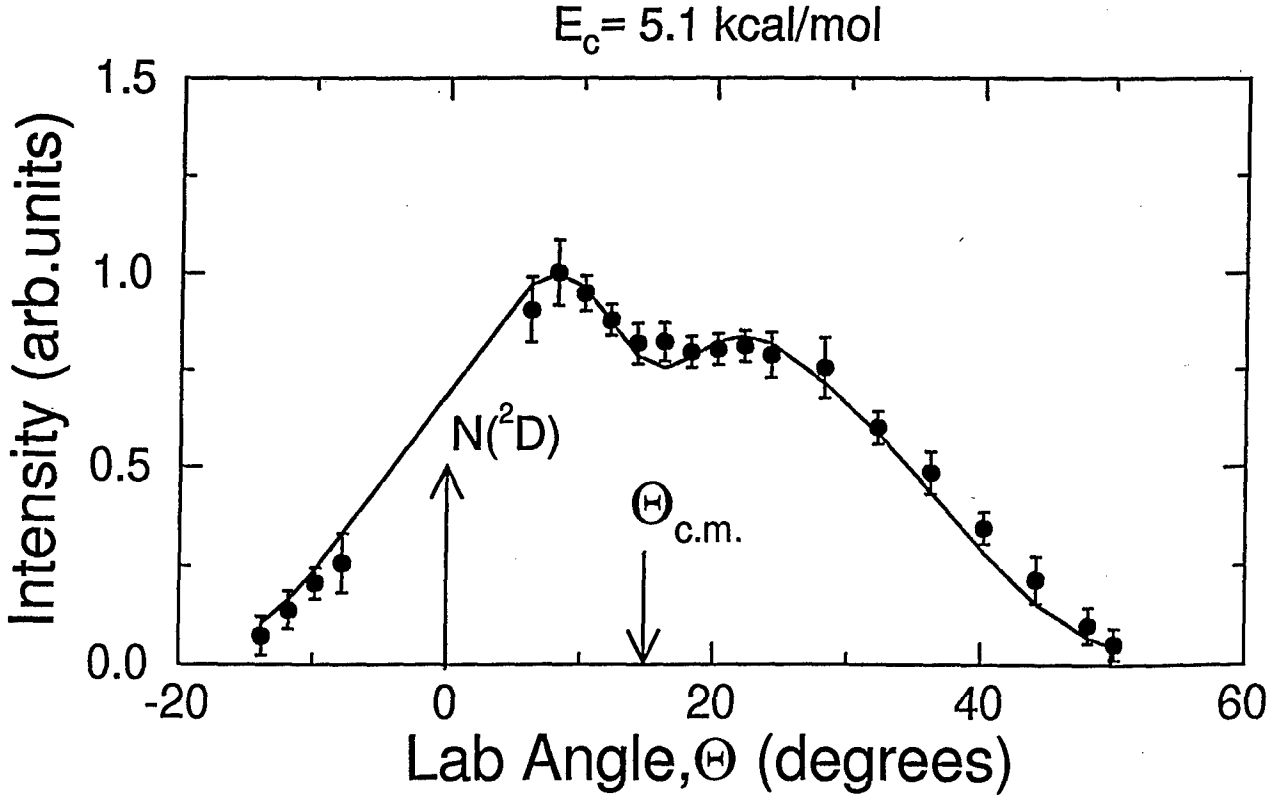

Fig. 12

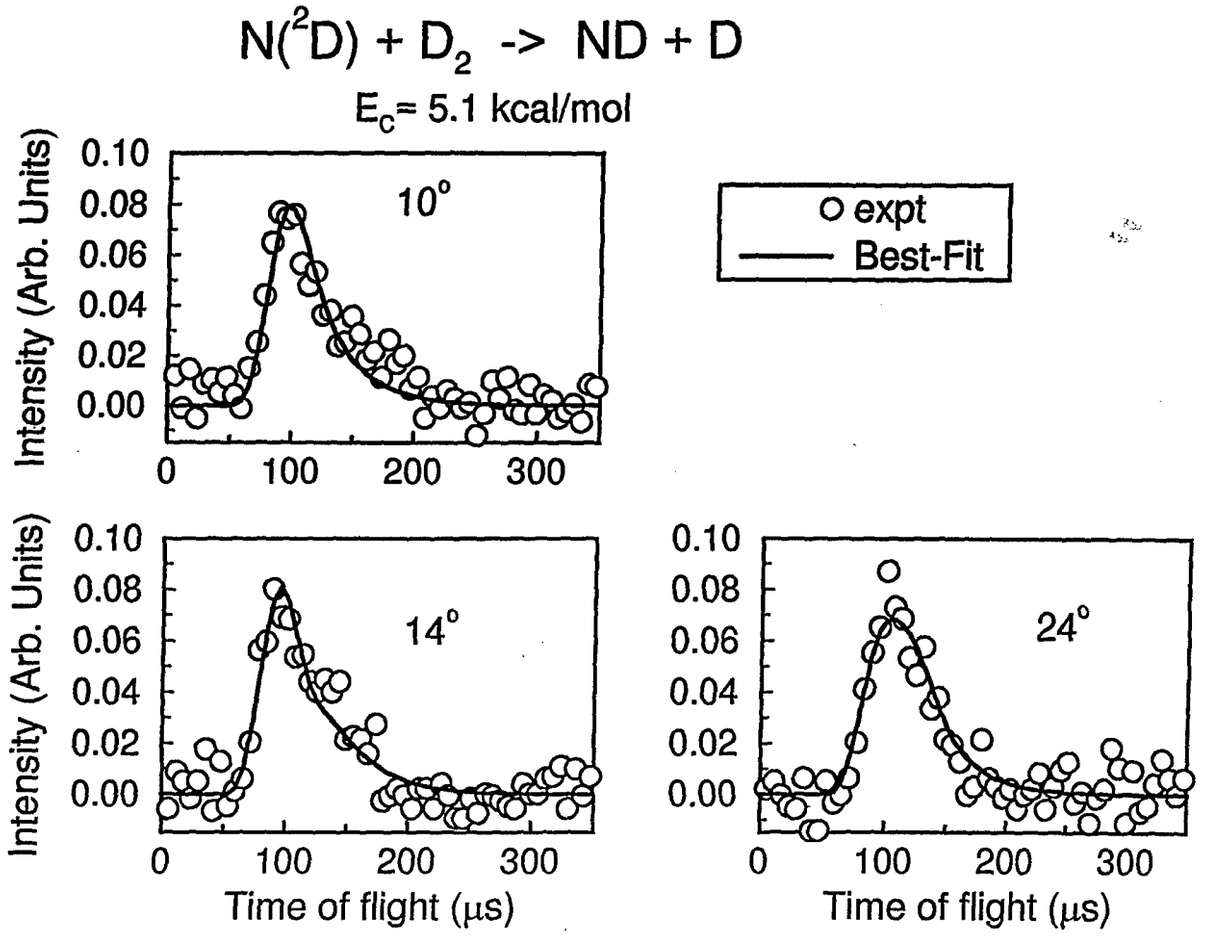
N(2D) + D2 -> ND + D
Ec= 5.1 kcal/mol
Intensity (Arb. Units)
0.10
0.08
0.06
0.04
0.02
0.00
10°
14°
24°
0
100
200
300
o expt
Best-Fit
Time of flight (μs)

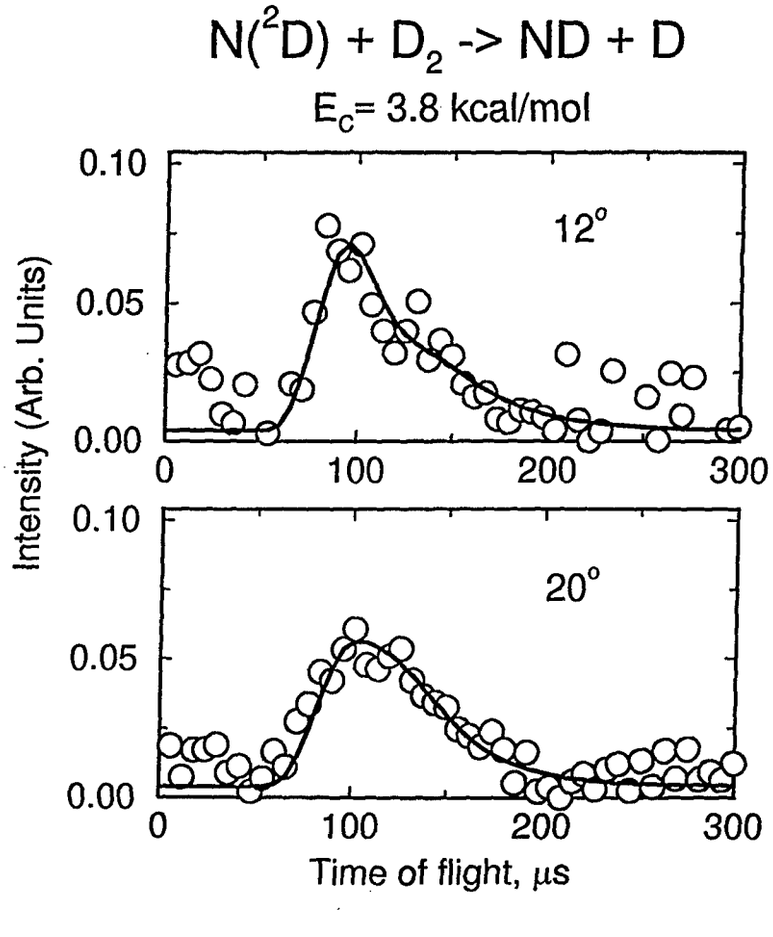
N(2D) + D2 -> ND + D
Ec= 3.8 kcal/mol
Intensity (Arb. Units)
0.10
0.05
0.00
12°
20°
0
100
200
300
Time of flight, μs

Fig. 13

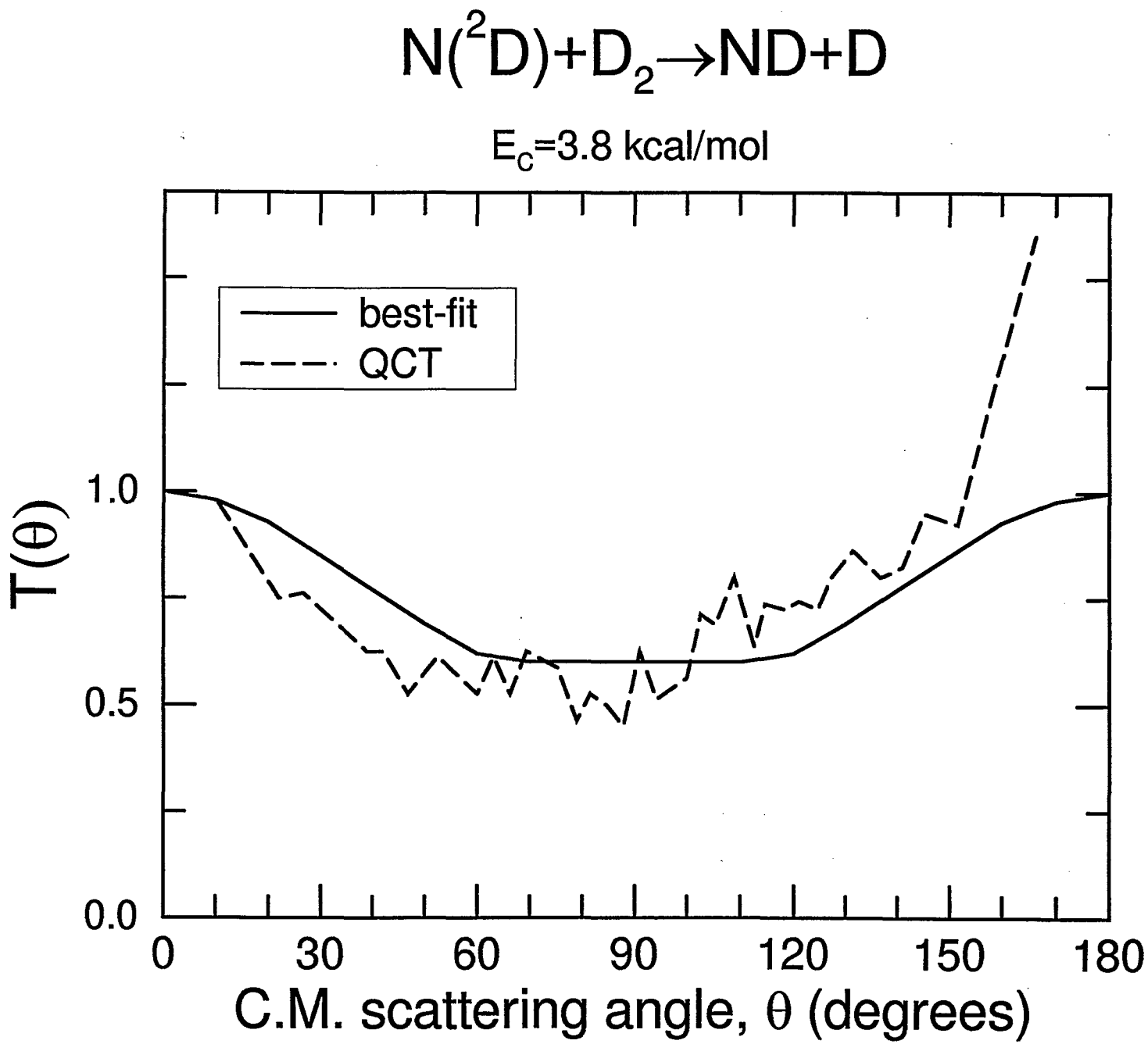
N(2D)+D2→ND+D
Ec=3.8 kcal/mol
best-fit
QCT
T(θ)
1.0
0.5
0.0
0
30
60
90
120
150
180
C.M. scattering angle, θ (degrees)

Fig. 14

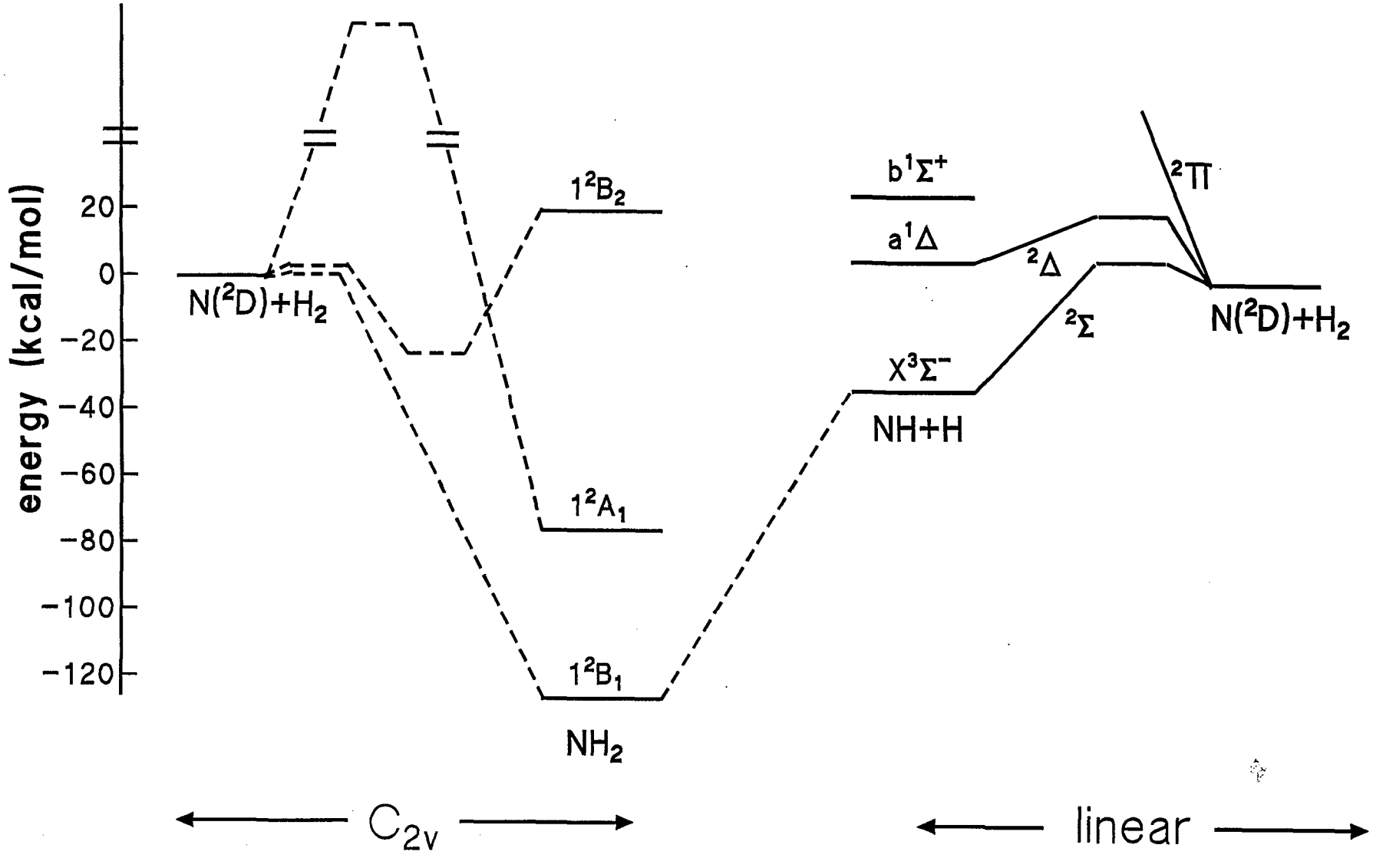
energy (kcal/mol)
20
0
−20
−40
−60
−80
−100
−120
N(²D)+H₂
1²B₂
1²A₁
1²B₁
NH₂
b¹Σ⁺
a¹Δ
²Π
²Δ
²Σ
X³Σ⁻
NH+H
N(²D)+H₂
C2v
linear

Fig. 15

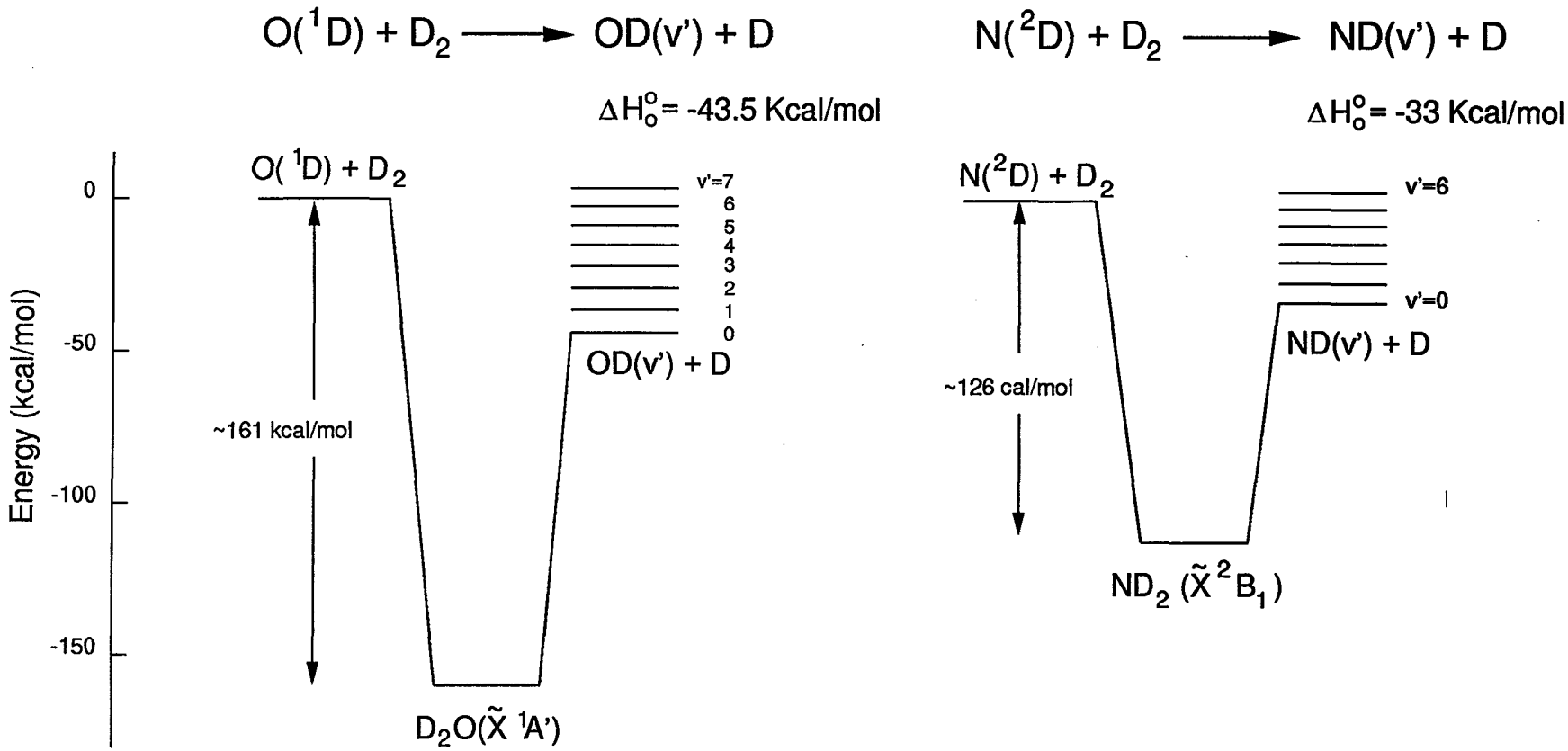
O(1D) + D2 → OD(v') + D
ΔHo= -43.5 Kcal/mol
Energy (kcal/mol)
0
-50
-100
-150
O(1D) + D2
v'=7
6
5
4
3
2
1
0
OD(v') + D
~161 kcal/mol
D2O(X̃ 1A')
N(2D) + D2 → ND(v') + D
ΔHo= -33 Kcal/mol
N(2D) + D2
v'=6
v'=0
ND(v') + D
~126 cal/mol
ND2 (X̃ 2B1)

Fig. 16

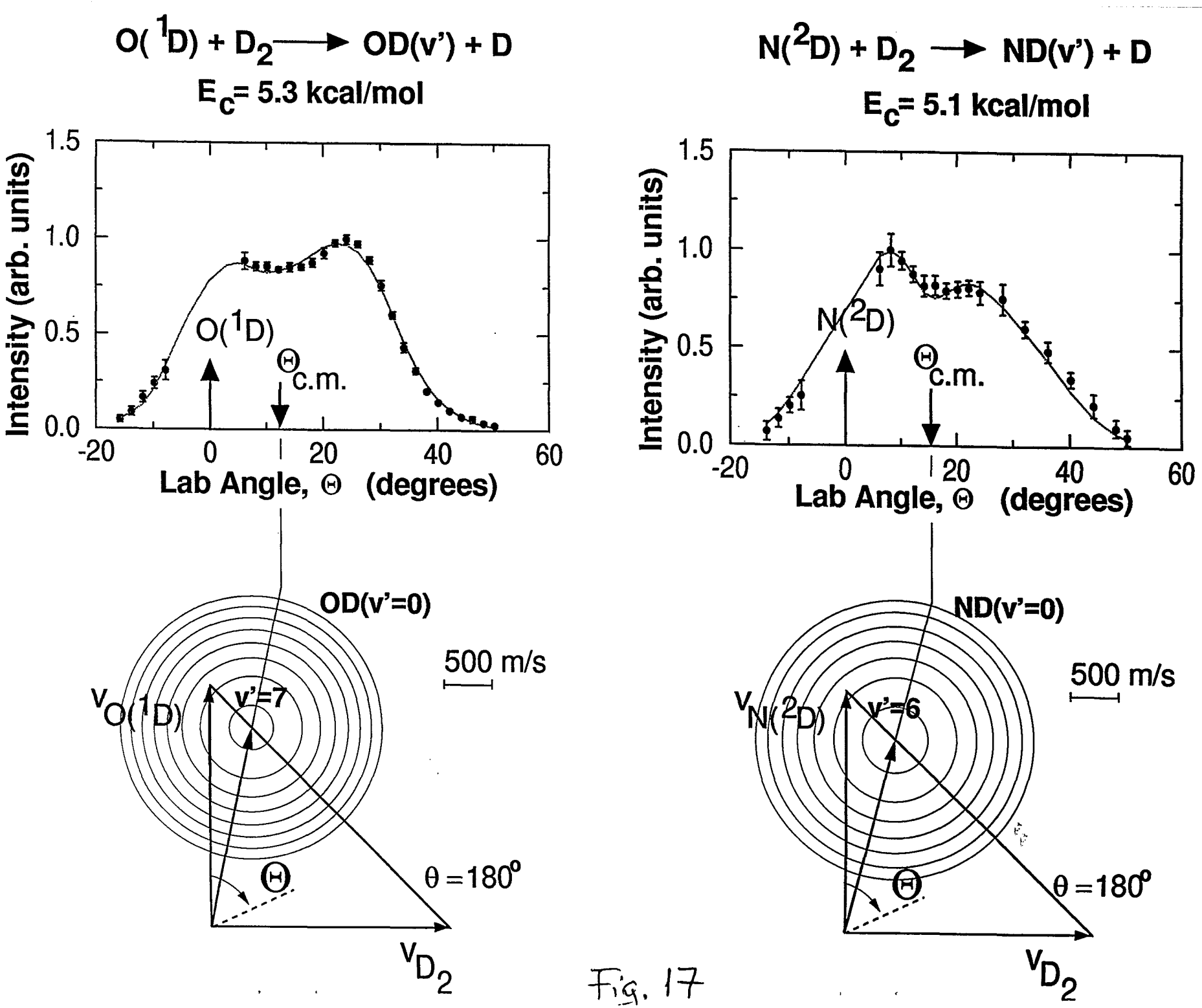
O(1D) + D2 → OD(v') + D
Ec= 5.3 kcal/mol
Intensity (arb. units)
1.5
1.0
0.5
0.0
-20
0
20
40
60
O(1D)
Θc.m.
Lab Angle, Θ (degrees)
OD(v'=0)
500 m/s
v'=7
vO(1D)
Θ
θ =180°
vD2
N(2D) + D2 → ND(v') + D
Ec= 5.1 kcal/mol
Intensity (arb. units)
1.5
1.0
0.5
0.0
-20
0
20
40
60
N(2D)
Θc.m.
Lab Angle, Θ (degrees)
ND(v'=0)
500 m/s
v'=6
vN(2D)
Θ
θ =180°
vD2

Fig. 17

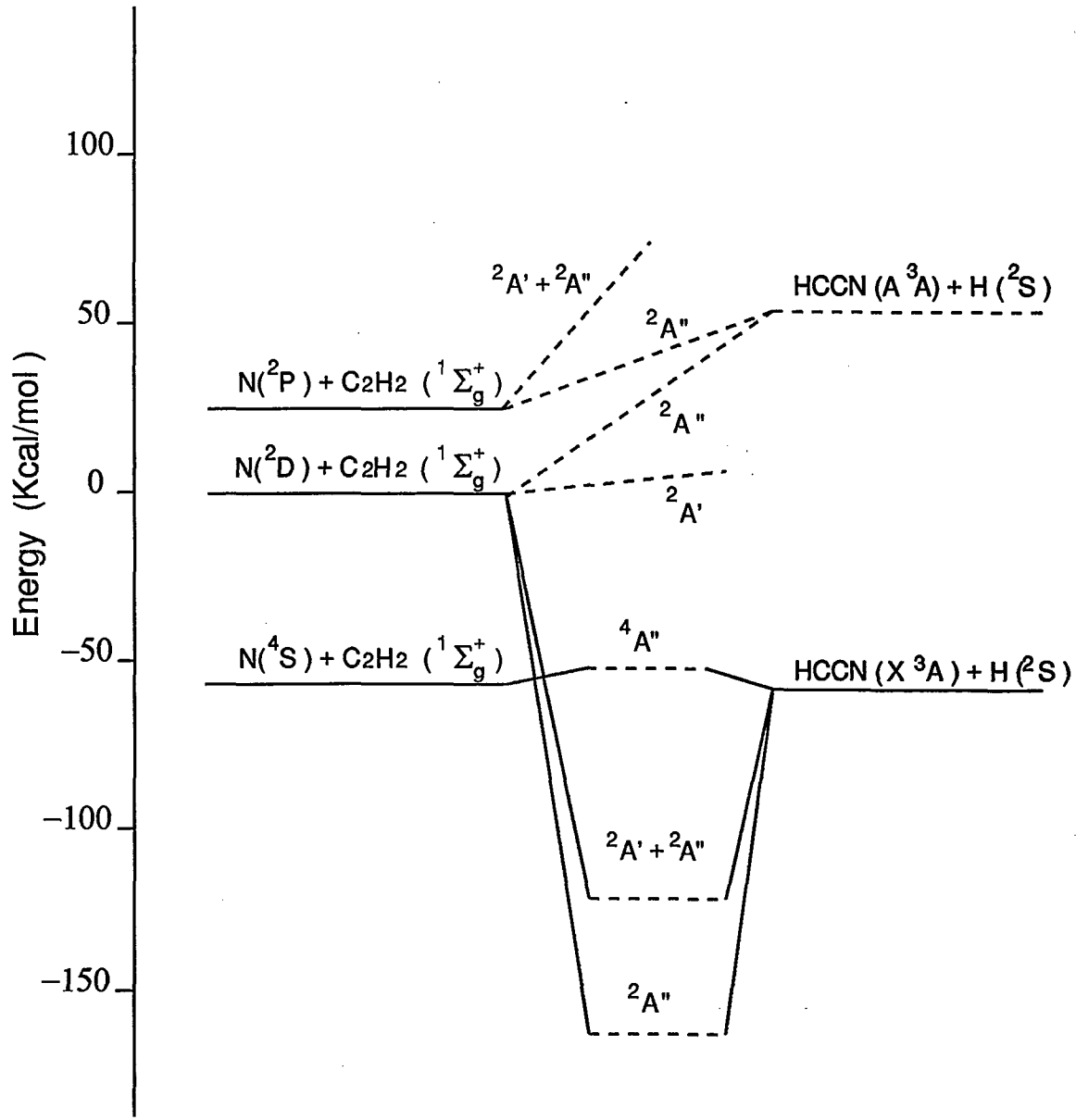
Energy (Kcal/mol)
100
50
0
−50
−100
−150
$^2A' + ^2A''$
HCCN ($A\ ^3A$) + H (^2S)
$^2A''$
$N(^2P) + C_2H_2\ (^1\Sigma_g^+)$
$^2A''$
$N(^2D) + C_2H_2\ (^1\Sigma_g^+)$
$^2A'$
$^4A''$
$N(^4S) + C_2H_2\ (^1\Sigma_g^+)$
HCCN ($X\ ^3A$) + H (^2S)
$^2A' + ^2A''$
$^2A''$

Fig. 18

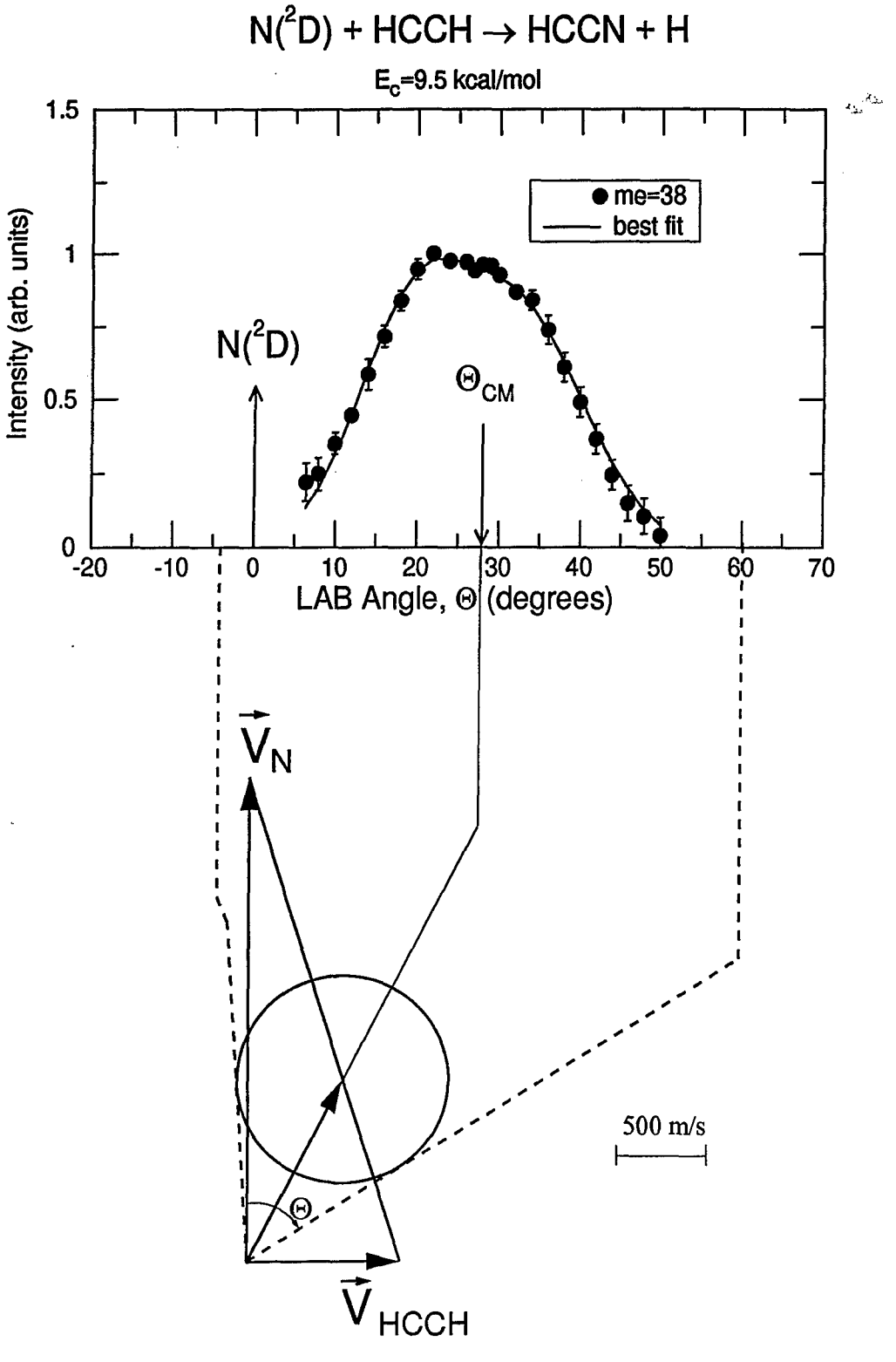
N(2D) + HCCH → HCCN + H
Ec=9.5 kcal/mol
me=38
best fit
Intensity (arb. units)
N(2D)
ΘCM
LAB Angle, Θ (degrees)
VN
VHCCH
Θ
500 m/s

Fig. 19

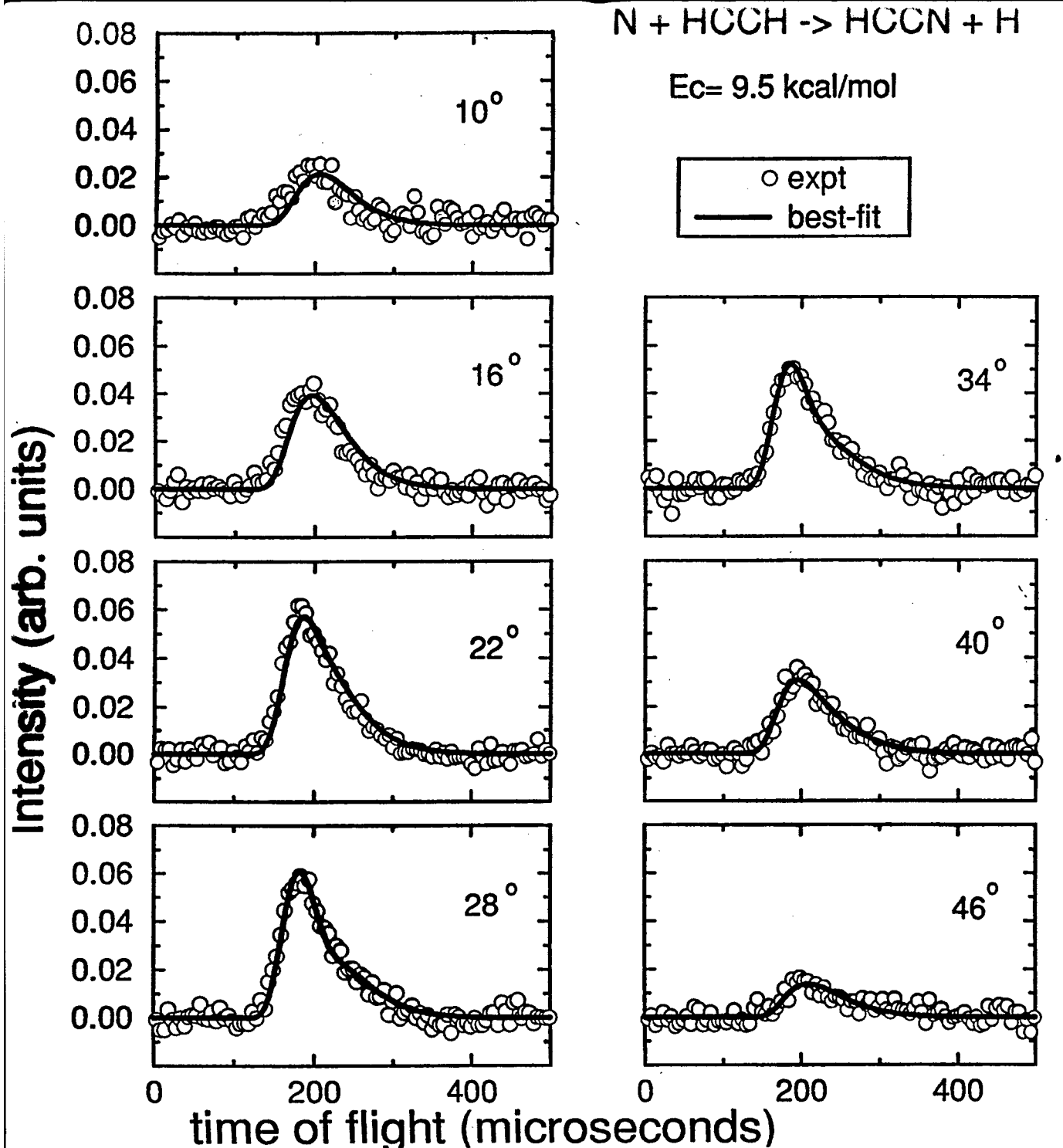

$N(^2D) + HCCH \longrightarrow \underline{HCCN} + H$

Time-of-flight distributions

Fig. 20

$N(^2D)+C_2H_4$

E_c=7.95 kcal/mol

LAB ANGULAR DISTRIBUTION

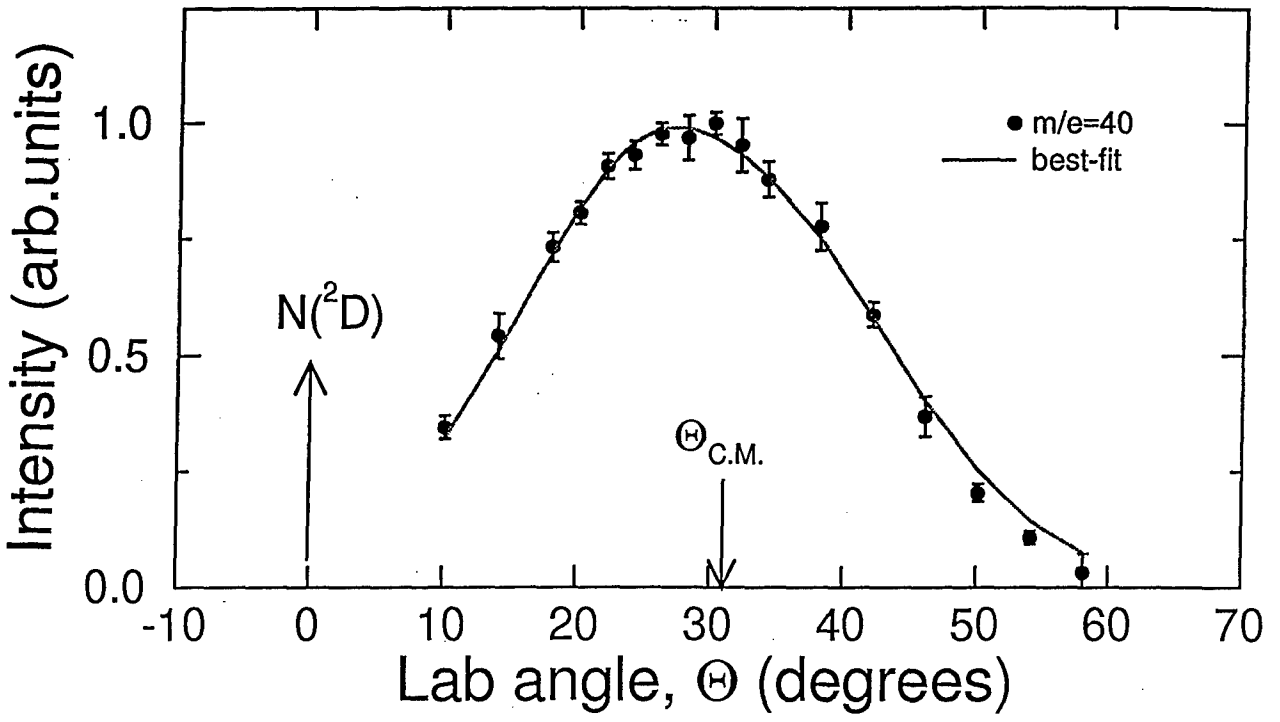

Time-of-flight Spectra

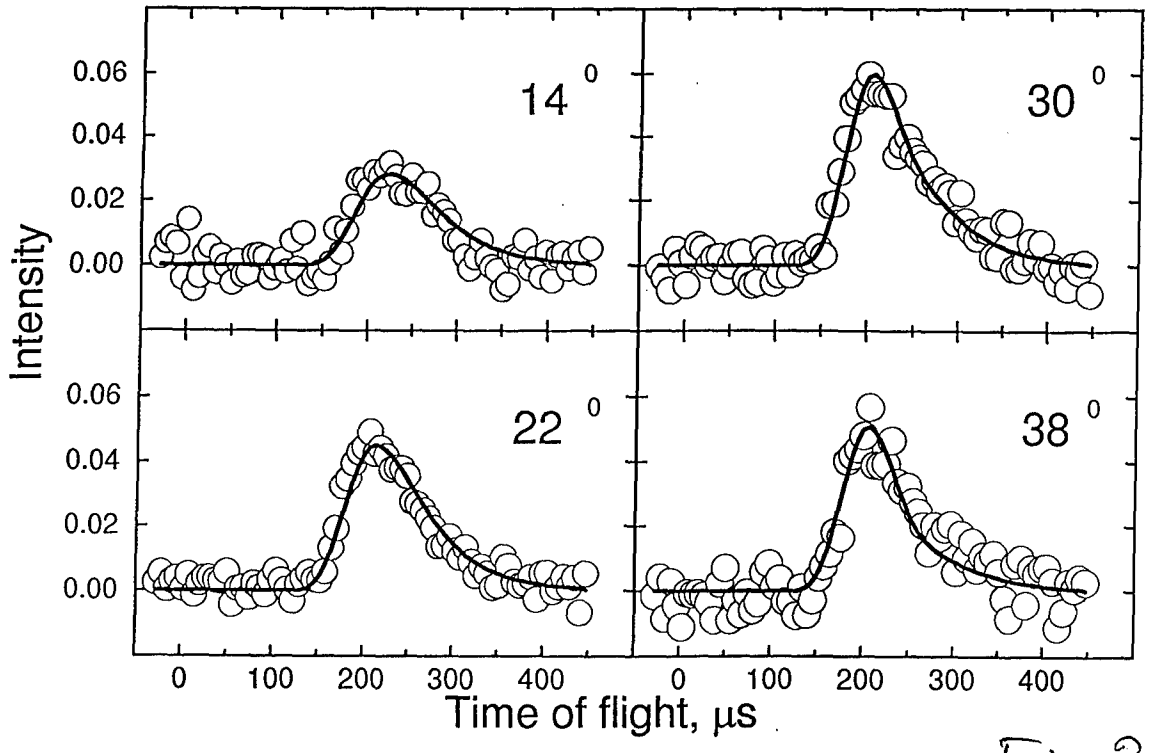

Fig. 21